PDE Transform --- a unified paradigm for image analysis and multiscale modeling

Guowei Wei

Department of Mathematics

Michigan State University

May 15, 2012, Shanghai JiaoTong University

June 1, 2012, Xidian University

Diffusion equation for image processing
(Withkin 1983)

$$u_t(r,t) = d\nabla^2 u(r,t)$$
$$u(r,0) = I(r)$$

Constant

Scale-space filter
Gaussian filter

Original

Original+Noise

Processed with the diffusion equation

Perona-Malik equation (1990)

$$\frac{\partial u}{\partial t} = \nabla \bullet \left[d\left(|\nabla u|\right) \nabla u \right],$$

$$u(r, t=0) = I(r)$$

Gradient dependent

$$d\left(|\nabla u|\right) = \exp\left(-\frac{|\nabla u|^2}{2\sigma^2} \right), \qquad or$$

$$d\left(|\nabla u|\right) = \frac{1}{1+|\nabla u|^2}$$

Mean Curvature Flow

Osher & Sethian (1998); Chan

Original

The first high-order stochastic geometric PDEs introduced for image analysis

Wei (IEEE SPL 1999); Greer & Bertozzi (2004); Gilboa, Sochen & Zeevi (2004); Xu and Zhou (2007); ....

$$\frac{\partial u}{\partial t} = \sum_{j=0} \nabla \bullet \left[d_j \left(|\nabla u| \right) \nabla \nabla^{2j} u \right] + V\left(|\nabla u| \right),$$

Gradient dependent

Nonlinear term

$$u(r, t=0) = I(r)$$

$$d_0\left(|\nabla u| \right) = \exp\left(-\frac{|\nabla u|^2}{2\sigma^2} \right),$$

Stochastic coef.

$$\sigma^2 = \overline{\left| \nabla u - \overline{\nabla u} \right|^2}$$

Use of Cahn-Hilliard type of potential

$$\frac{\partial u}{\partial t} = \nabla \bullet \left[d_1(|\nabla u|) \nabla \nabla^2 u \right] + c(|\nabla u|)(u^2 - u_0^2)u$$

The first PDE based nonlinear high-pass filter

$$\frac{\partial u}{\partial t} = \nabla \bullet \left[d_u \left(|\nabla u| \right) \nabla u \right] + c_u (v - u),$$

$$\frac{\partial v}{\partial t} = \nabla \bullet \left[d_v \left(|\nabla v| \right) \nabla v \right] + c_v (u - v)$$

Relative fidelity

$$u(r, t = 0) = v(r, t = 0) = I(r)$$

$$Edge(E):$$

$$E(r,t) = u(r,t) - v(r,t)$$

Wei & Jia (EPL 2002); Sun,Wu,Wang & Wei (2006)

Original

Coupled PDEs

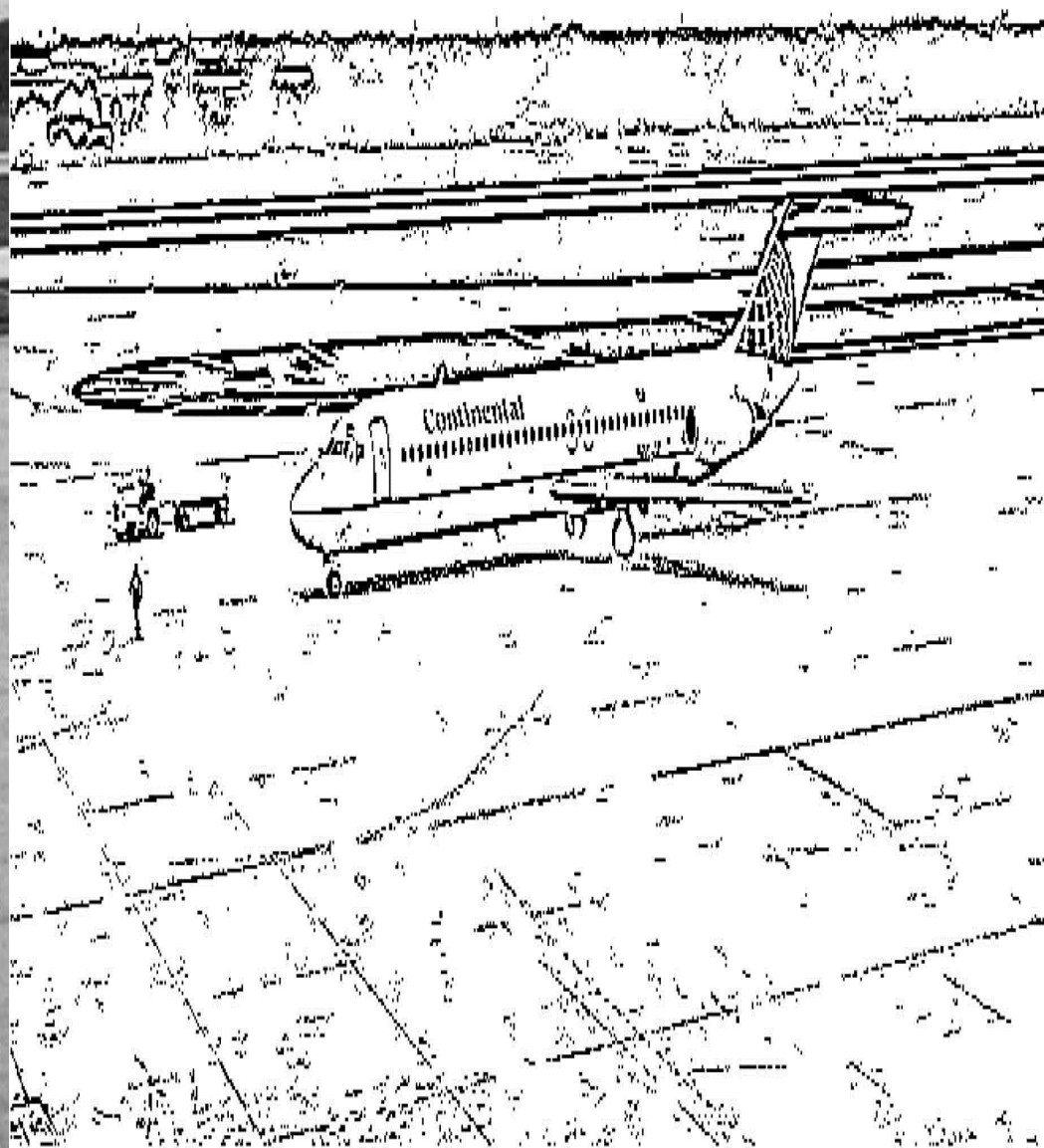

Edge detection using coupled PDEs

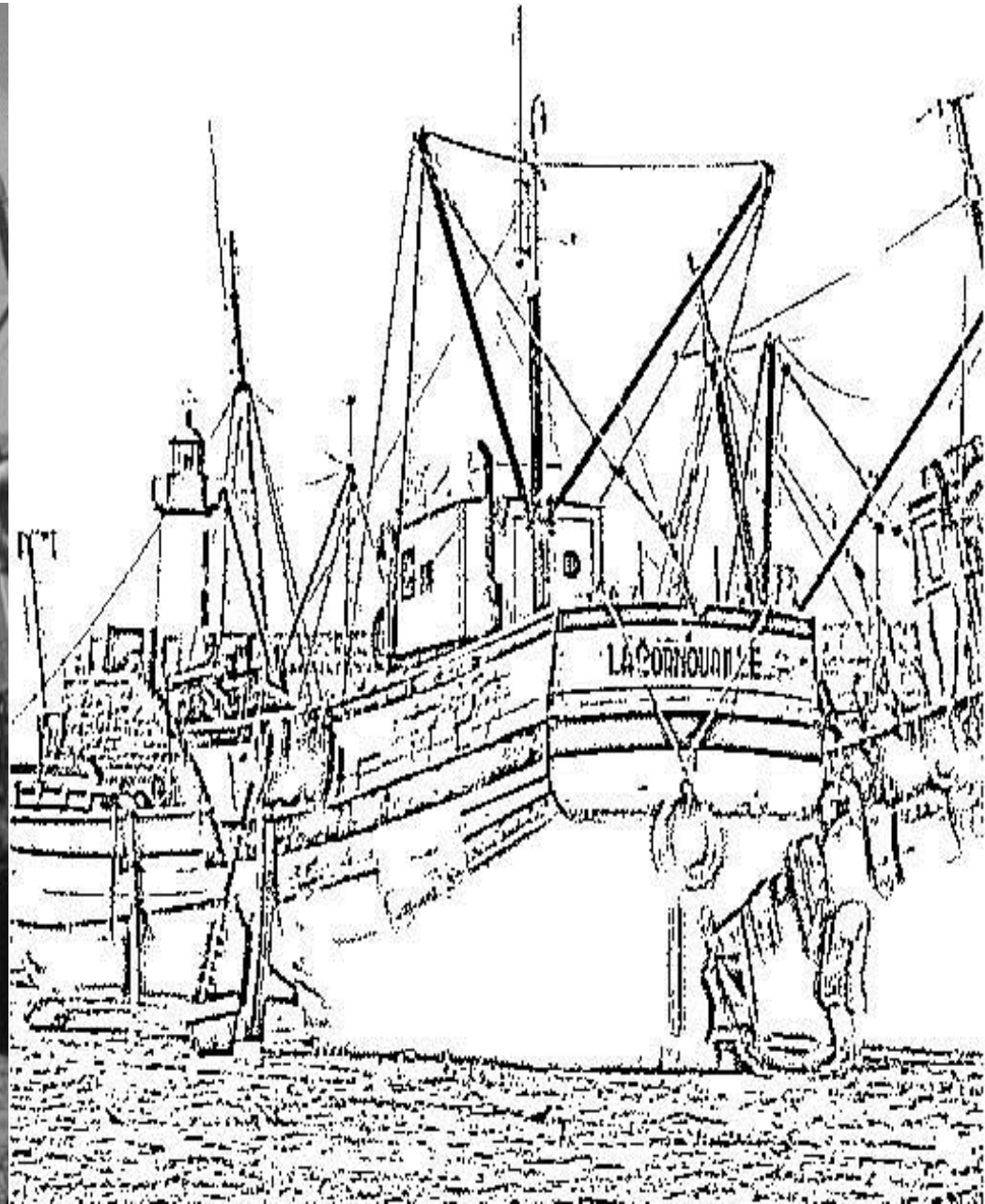

PDE transform

$$\frac{\partial u}{\partial t} = \sum_{i=0}^{n-1} \nabla \bullet \left[d_i \left(|\nabla u| \right) \nabla \nabla^{2i} u \right] + c_u (v - u),$$

$$\frac{\partial v}{\partial t} = \sum_{j=0}^{m-1} \nabla \bullet \left[d_j \left(|\nabla v| \right) \nabla \nabla^{2j} u \right] + c_v (u - v)$$

Wang, Wei, Yang, IJNMBE 2011

$$u(r, t = 0) = v(r, t = 0) = I(r)$$

Intrinsic mode functions (IMFs)

$$w_{nm}^k = u_n - v_m = H_{nm} X^k, \qquad \forall k = 1,2,...$$

$$X_{nm}^1 = I(r)$$

$$X_{nm}^k = X_{nm}^1 - \sum_{l=1}^{k-1} w_{nm}^l, \qquad \forall k = 2,3,...$$

$$I = X_{nm}^k + \sum_{l=1}^{k-1} w_{nm}^l$$

Perfect reconstruction

Frequency response of the PDE transform

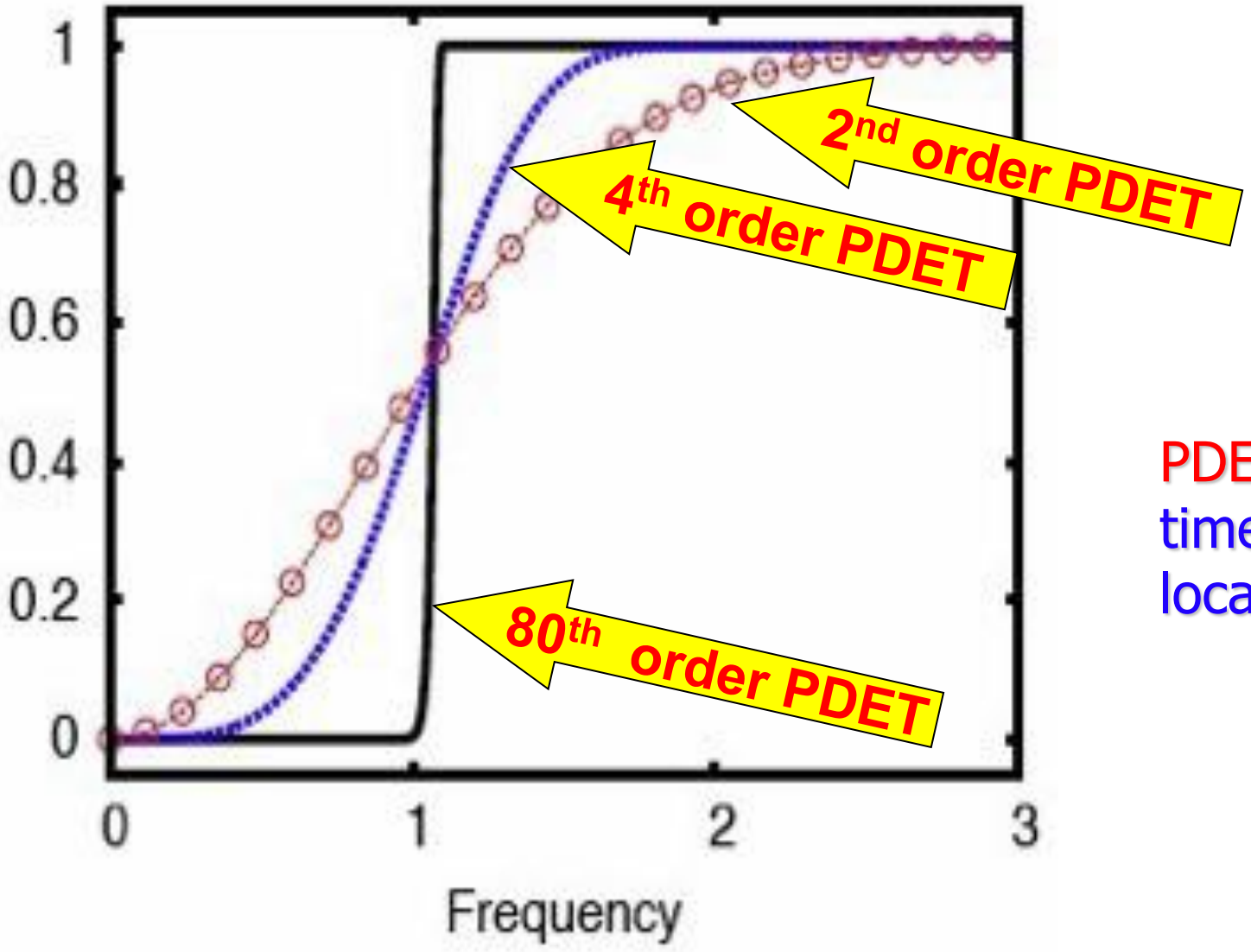

PDE order controls time-frequency localization

PDE transform for the processing of Cryo-EM data

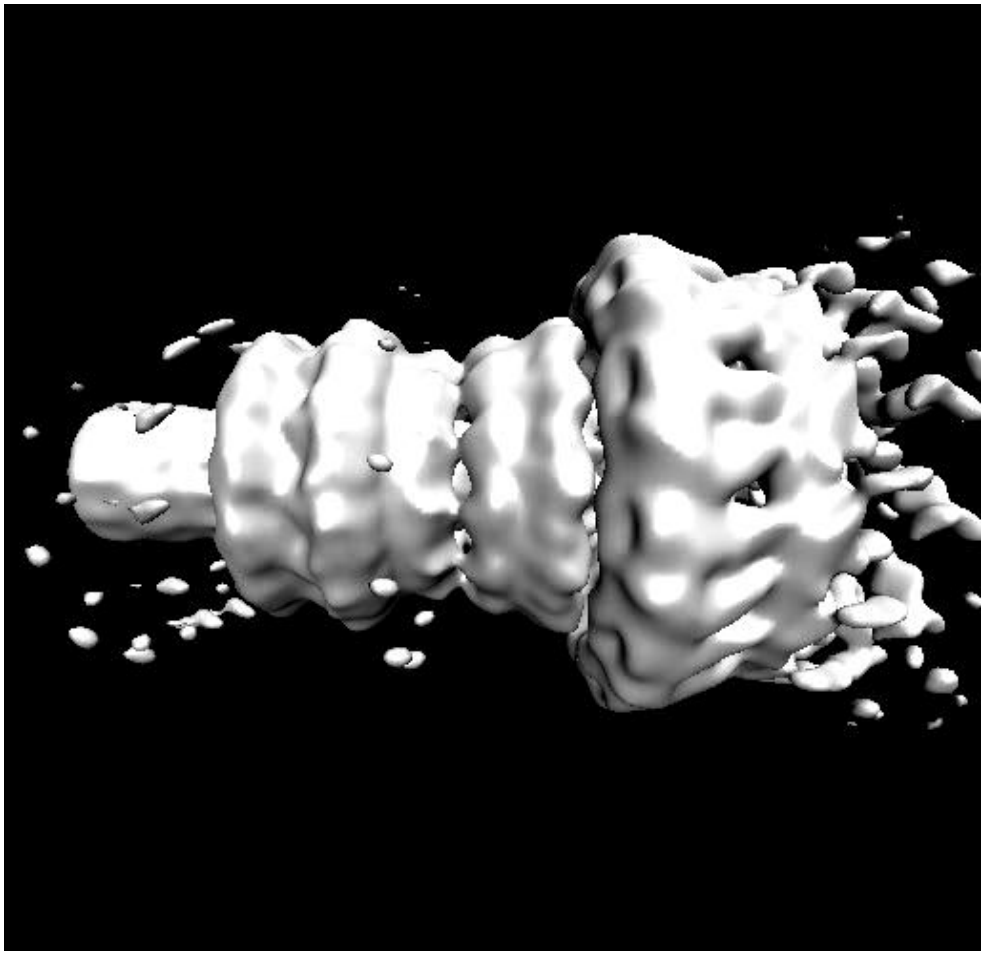

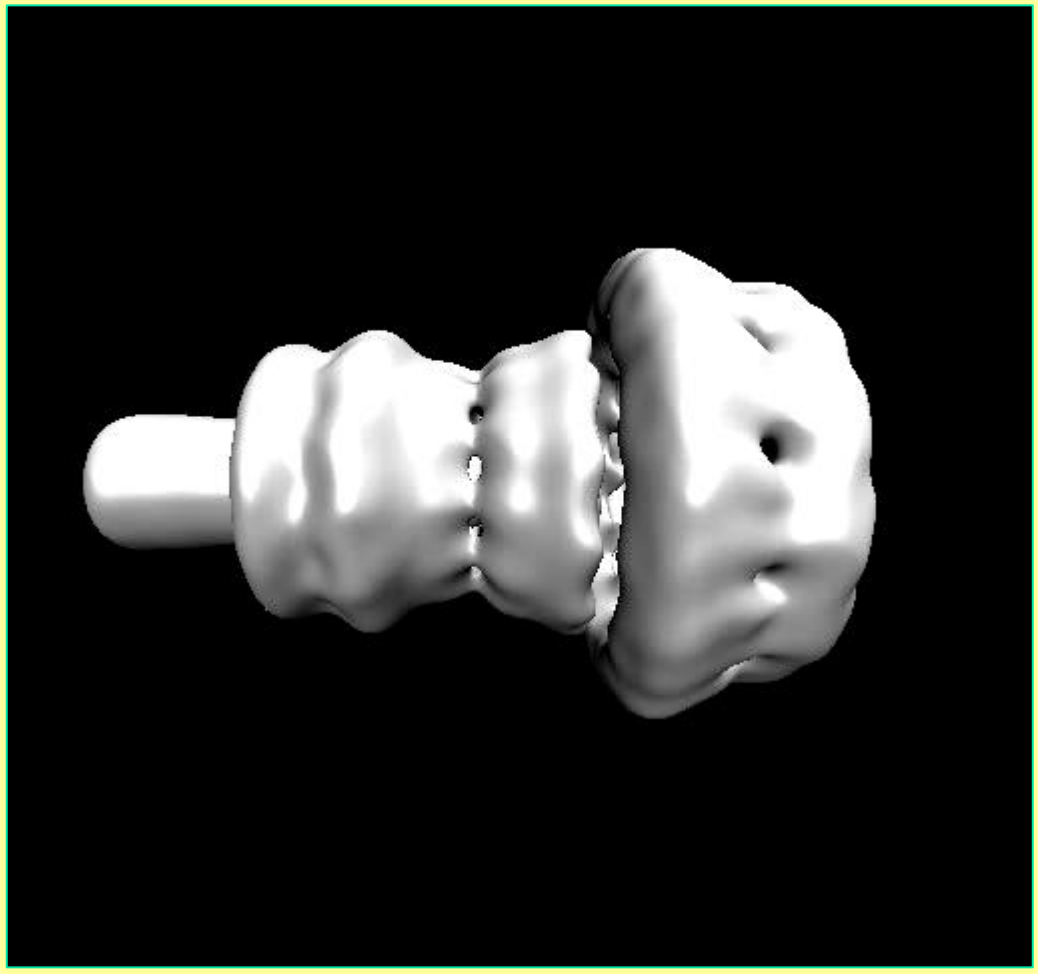

Bacterium Type III secretion system

Central Pacific sea surface temperature

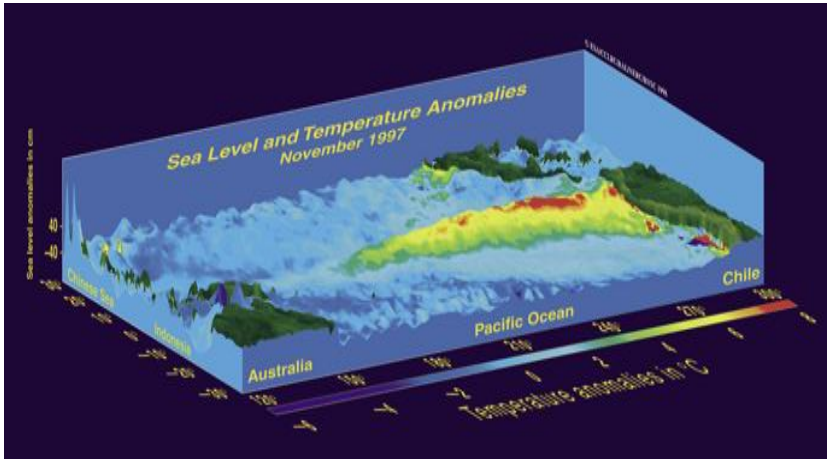

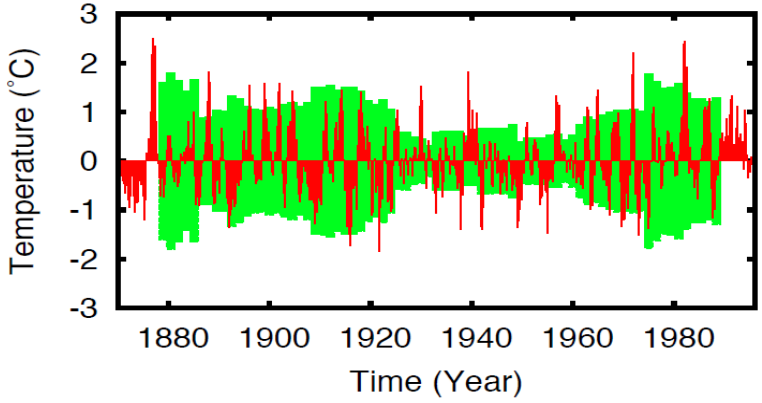

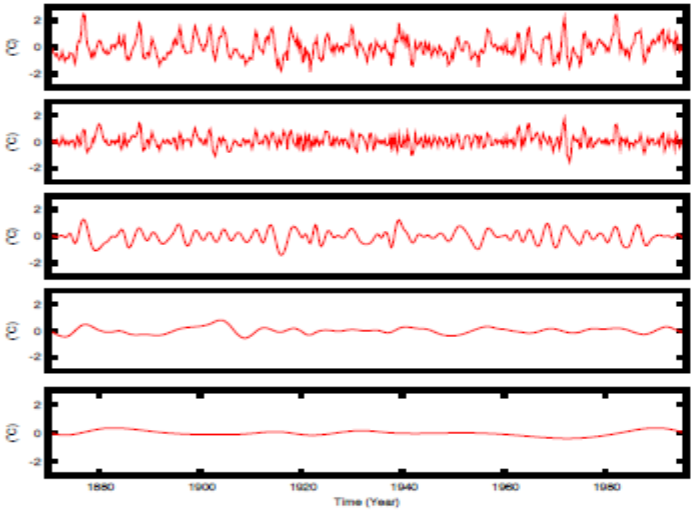

(a) The original SST signal (top panel) and the first four significant intrinsic mode functions generated by the EMD method.

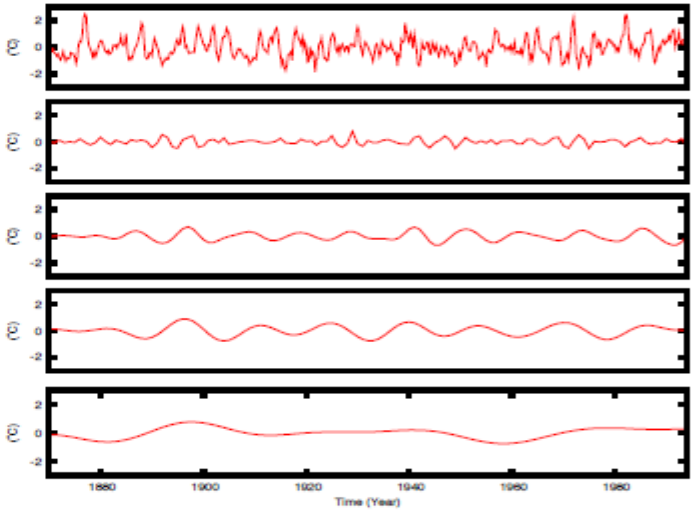

(b) The four modes generated by the PDE transform for the same SST signal on the top panel are similar to those from the EMD decomposition.

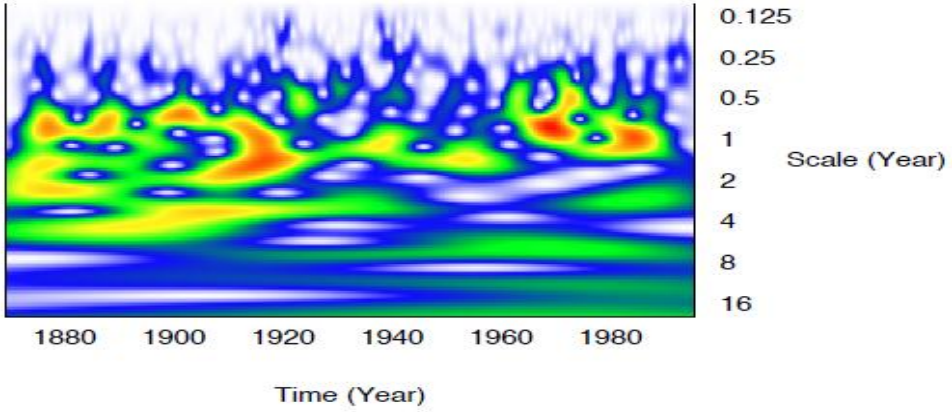

(a) Continuous wavelet analysis of the SST Nino3 data.

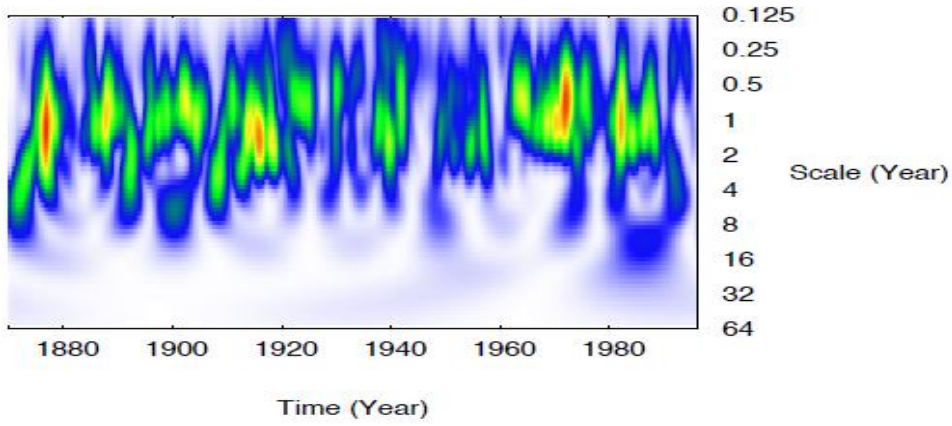

(b) PDE transform using 2nd order PDE.

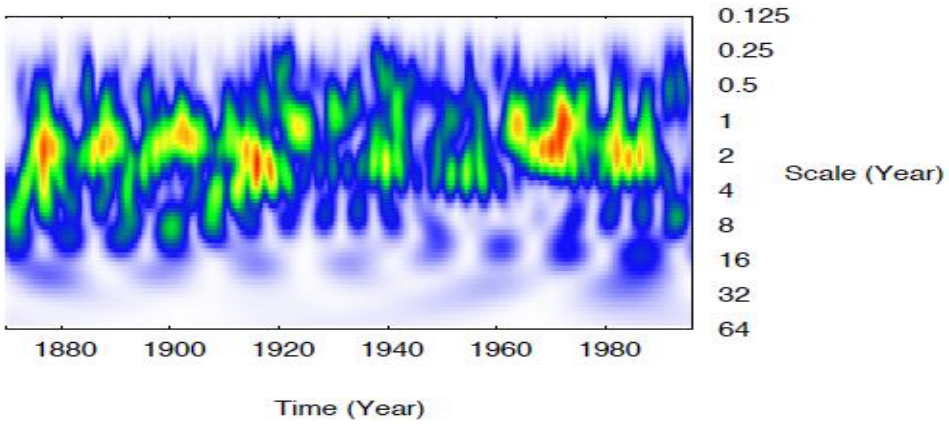

(c) PDE transform using 4th order PDE.

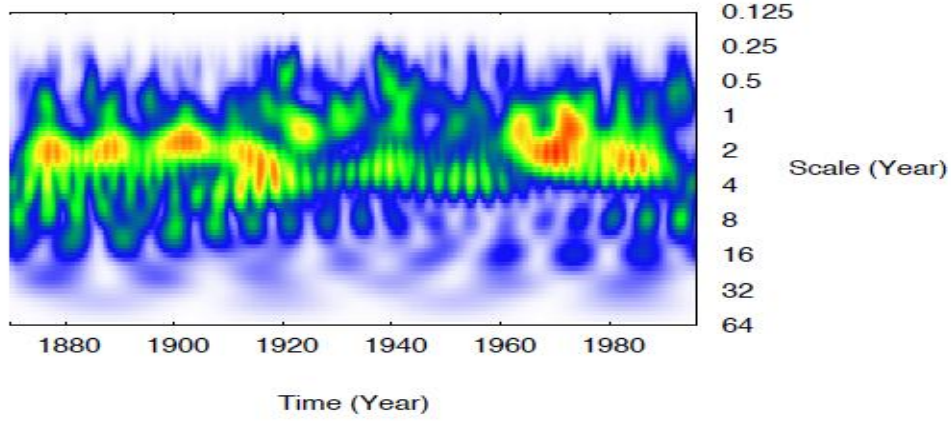

(d) PDE transform using 8th order PDE.

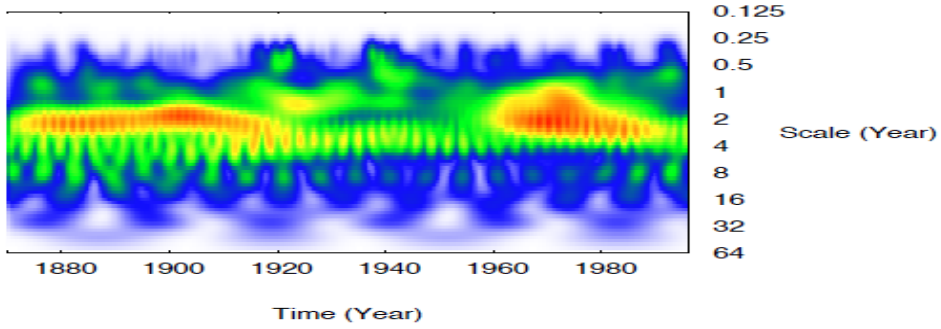

(e) PDE transform using 20th order PDE.

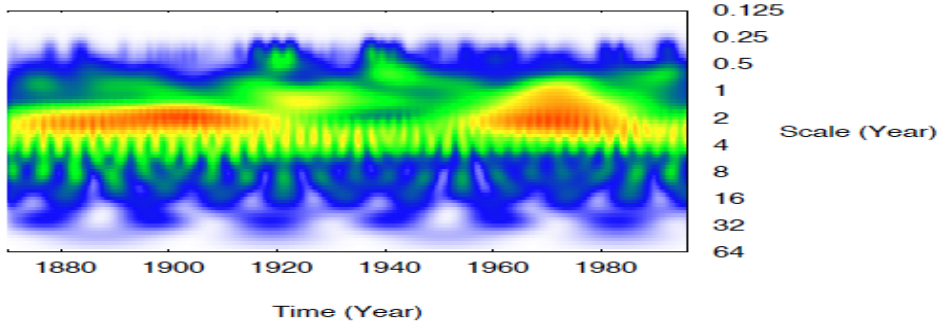

(f) PDE transform using 40th order PDE.

Wavelet transform vs PDE transform

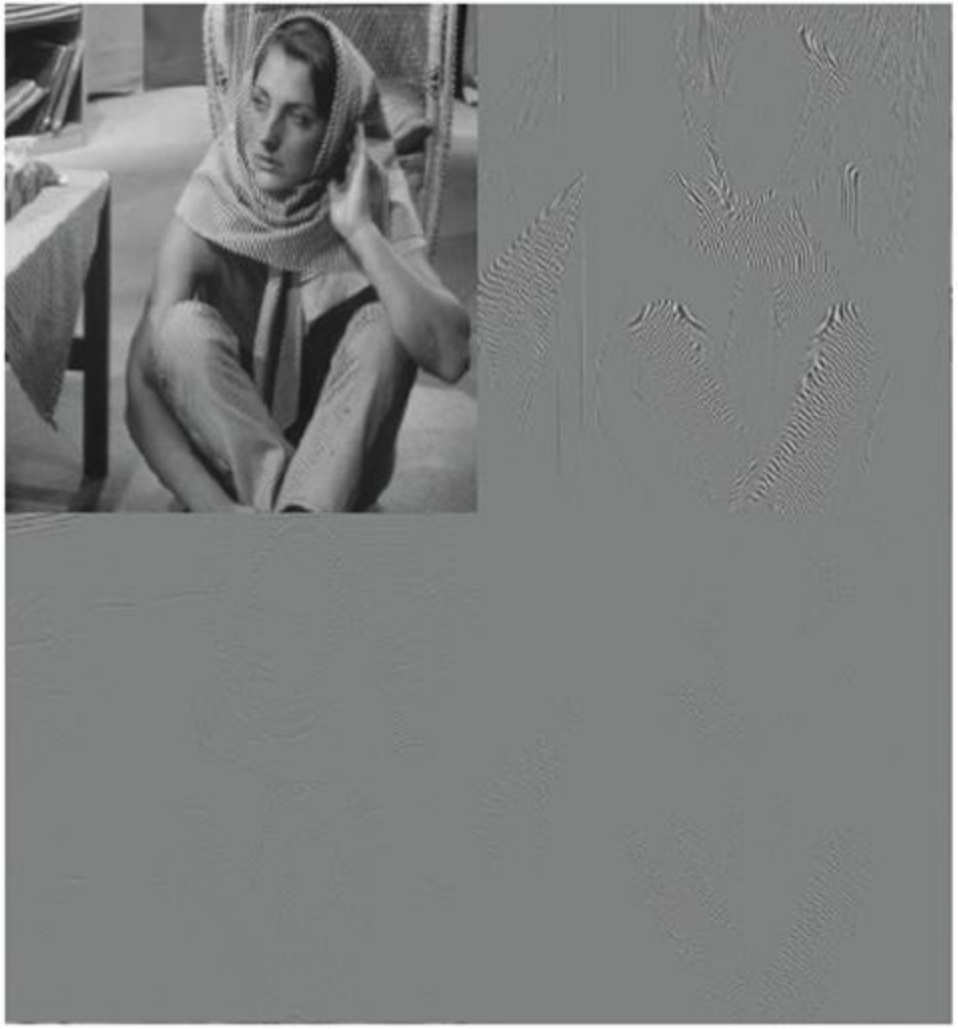

Wavelet transform

PDE transform

Adaptive PDE transform based local statistical analysis

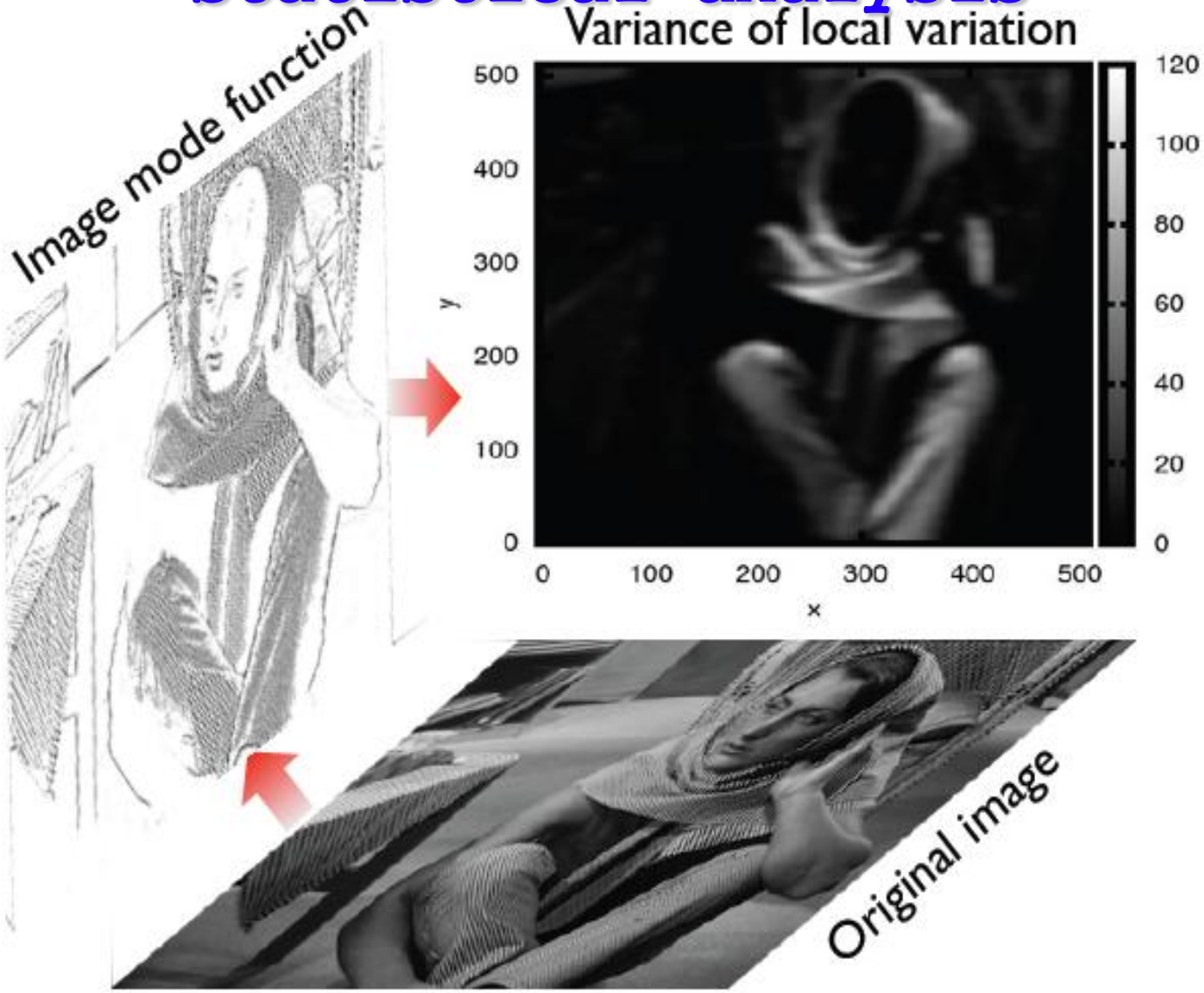

Figure 4: Adaptive PDE transform for selective texture extraction in the Barbara image. The variance of the local variation is shown in the top chart.

PDE transform based correlations

(a) Original Barbara image.

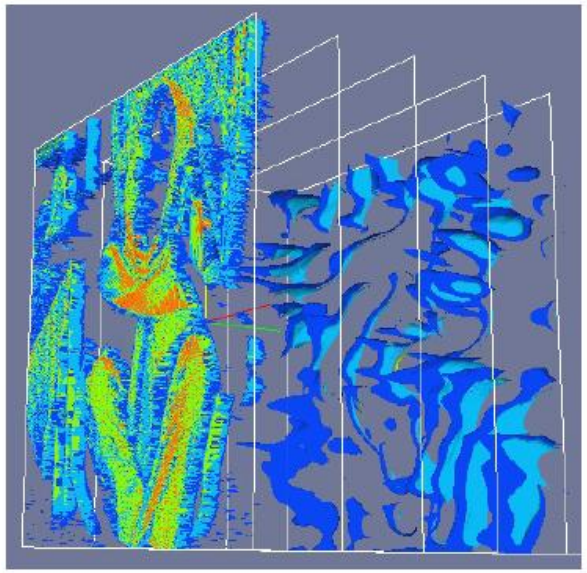

(b) 4D density of the Barbara image.

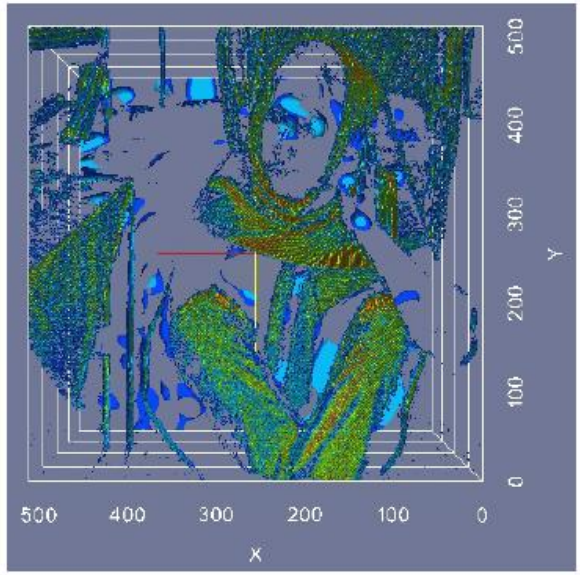

(c) Front view of the Figure 8(b).

(d) Original camera man image.

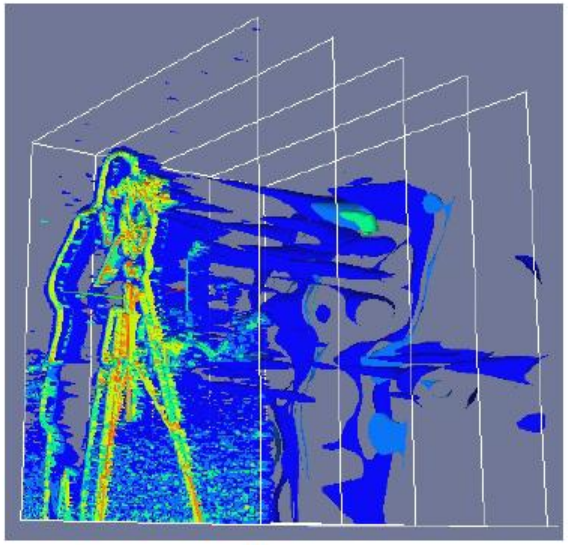

(e) 4D density of the camera man image.

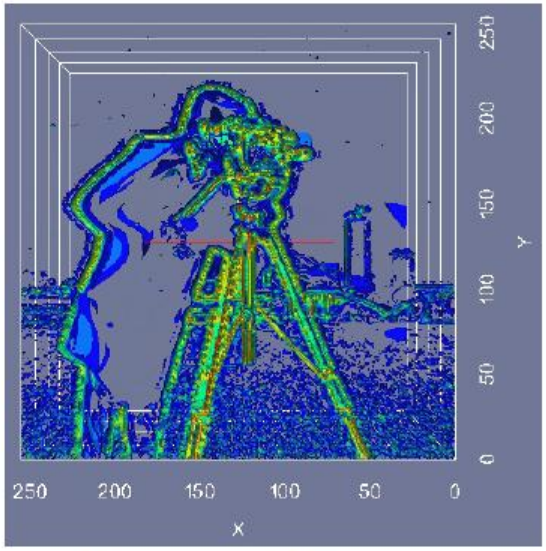

(f) Front view of the Figure 8(e).

(a) Original image.

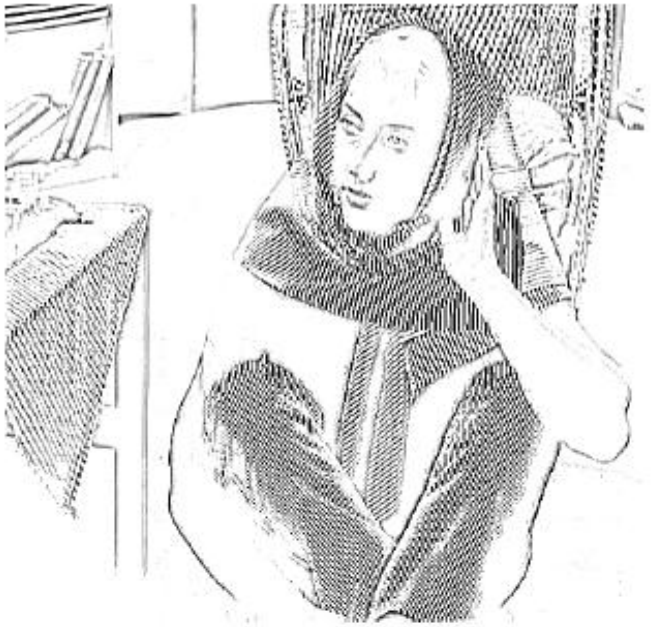

(b) Image mode function.

(c) Texture 1

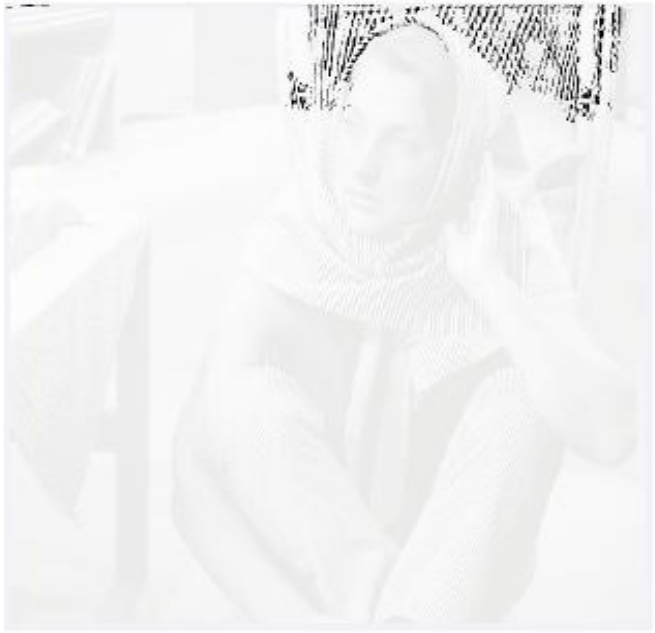

(d) Texture 2

Adaptive PDE transform for texture analysis

Wang, Wei, Yang, 2012

(a) Original image.

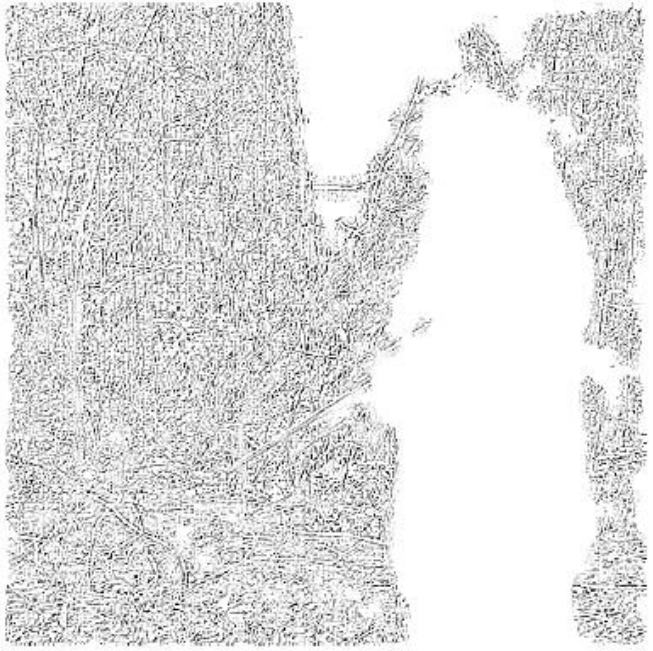

(b) Texture 1

(c) Texture 2

(d) Texture 3

Adaptive PDE transform for sniper identification

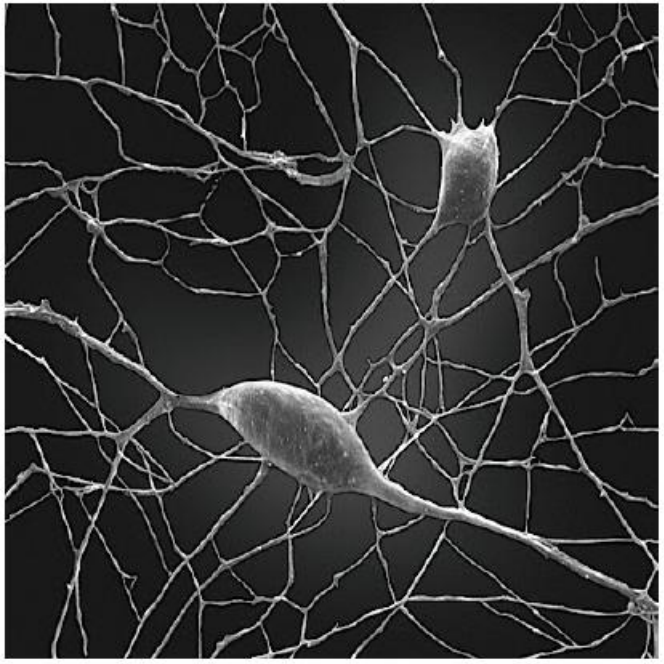

(a) Original neuron image.

(b) Class 1 of the selective neuron skeleton.

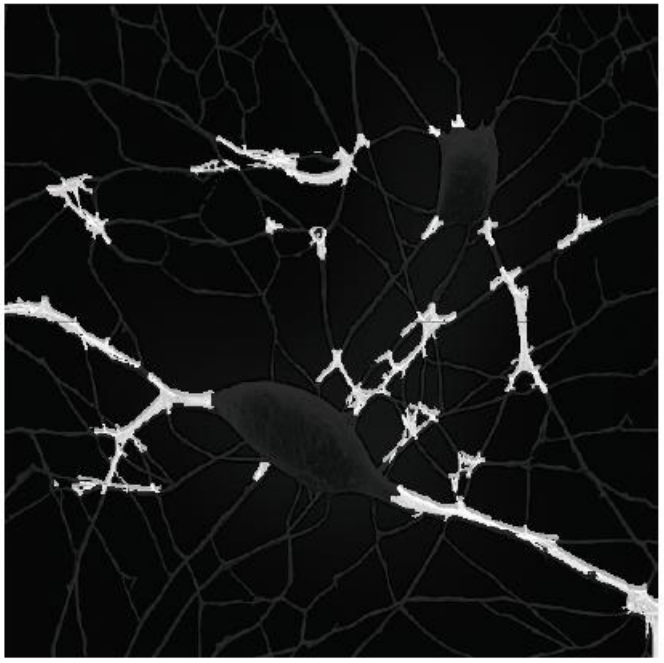

(c) Class 2 of the selective neuron skeleton.

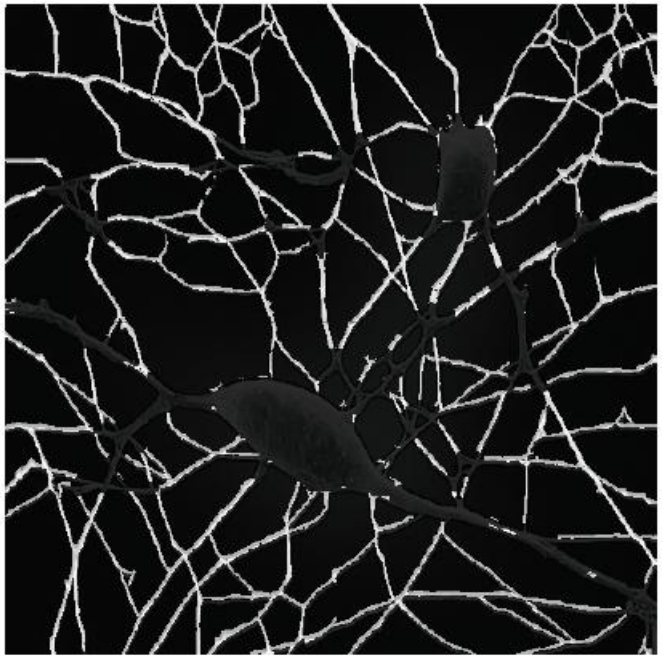

(d) Class 3 of the selective neuron skeleton.

Adaptive PDE transform for neuron classification

PDET for hyperbolic conservation laws

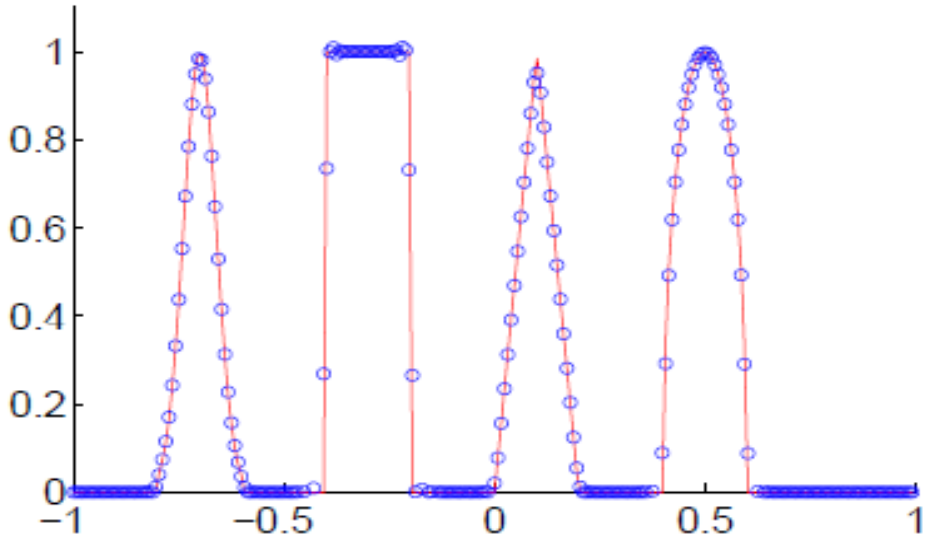

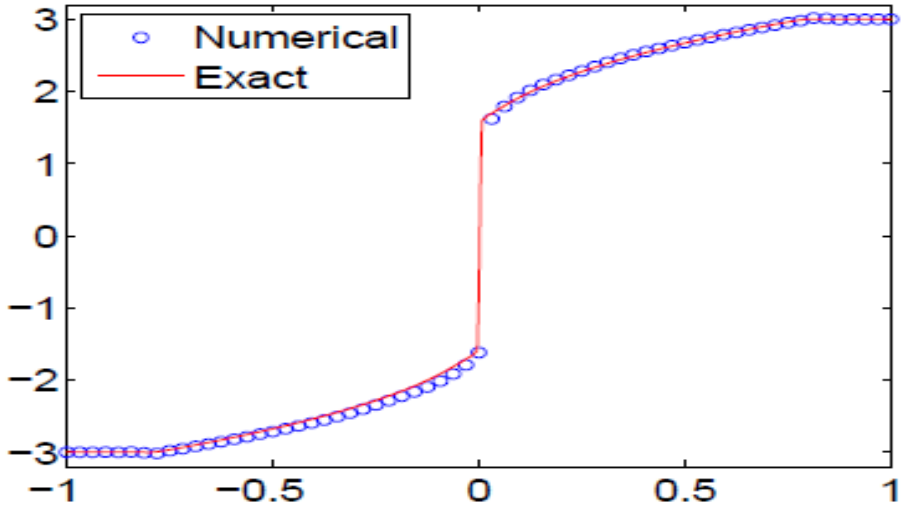

(c) The 6th order PDE transform (65 grid points)

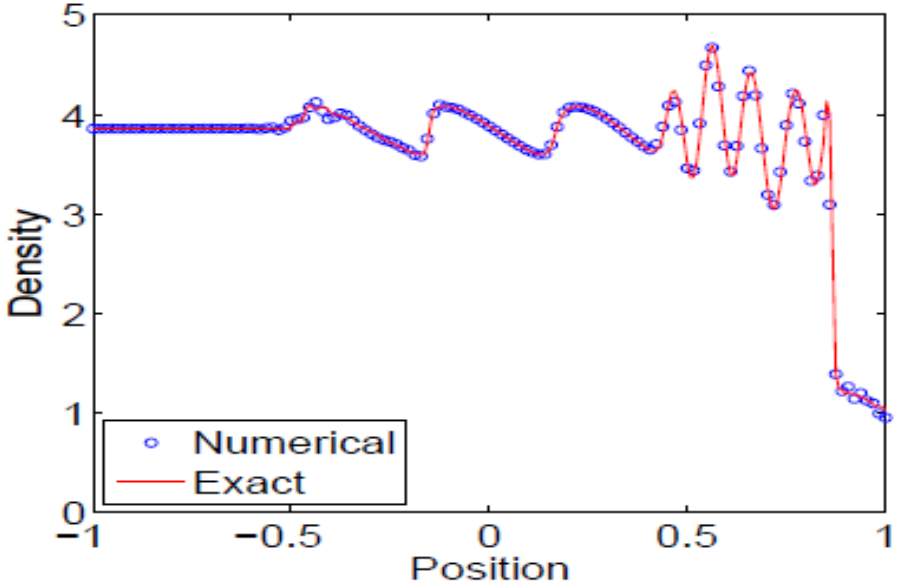

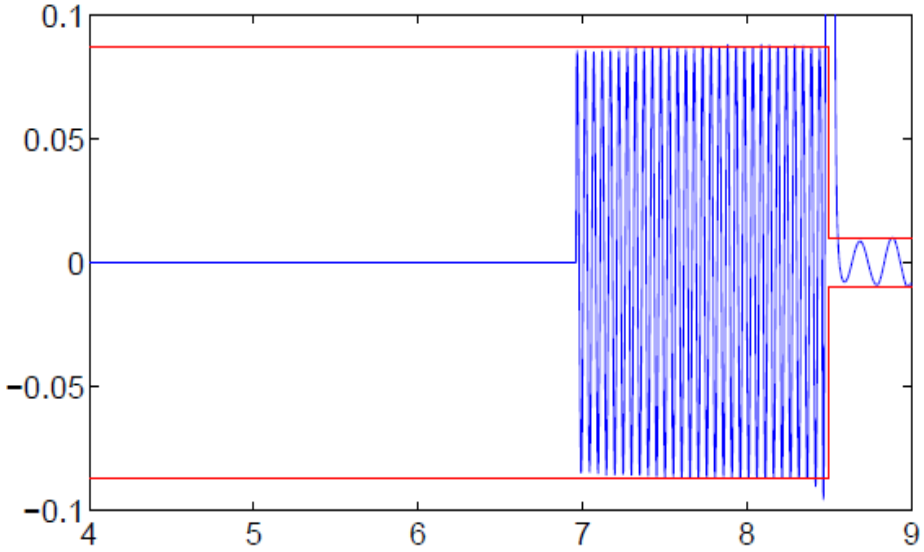

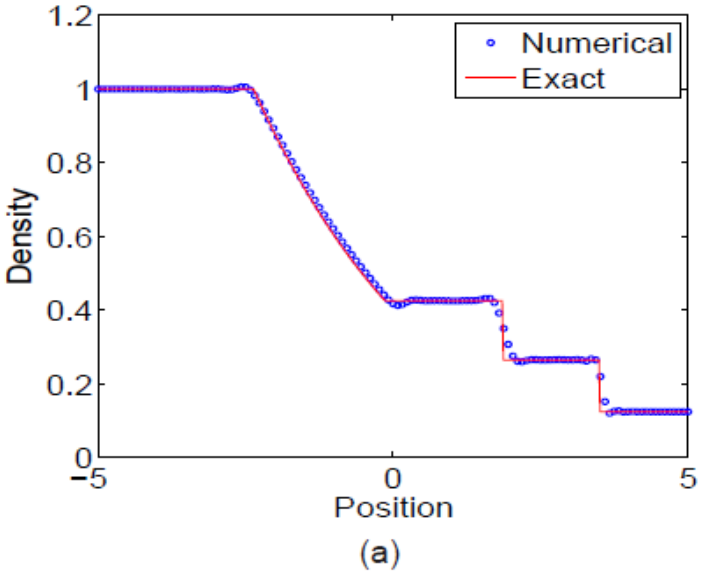

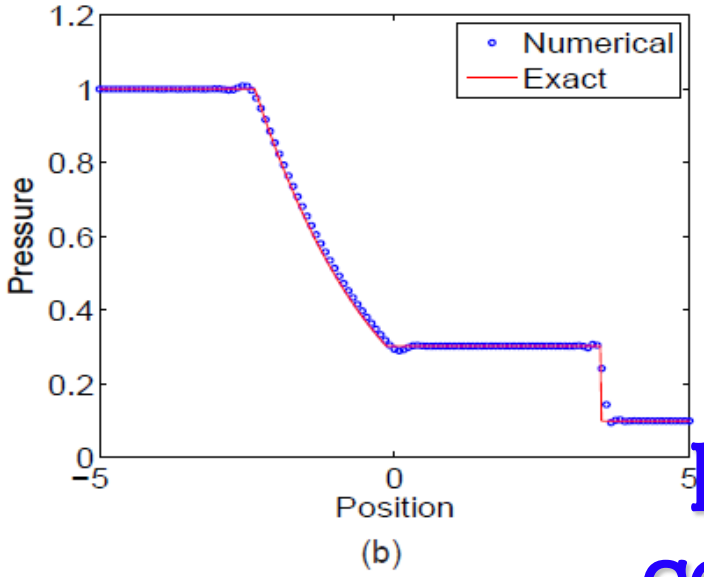

Figure 6: Numerical results from the 6th-order PDE transform for Sod's problem ($t = 1.5$, $\Delta t = 0.02$, 129 grid points). (a) Density; (b) Pressure.

PDE transform for hyperbolic conservation laws

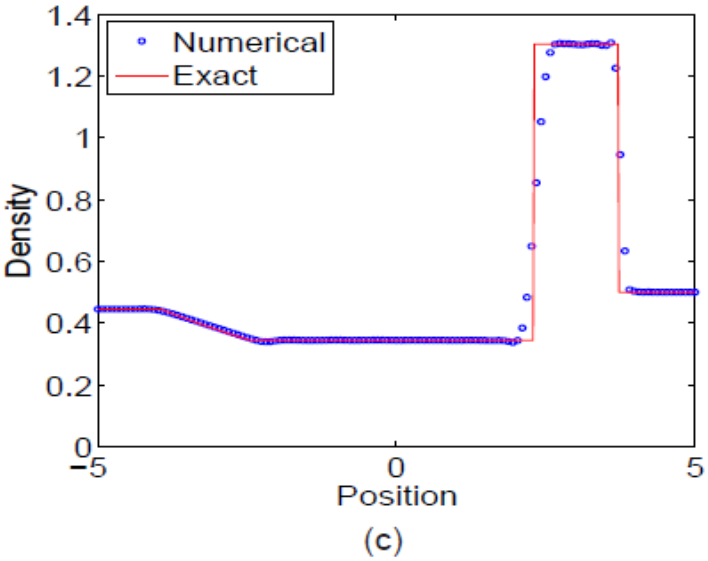

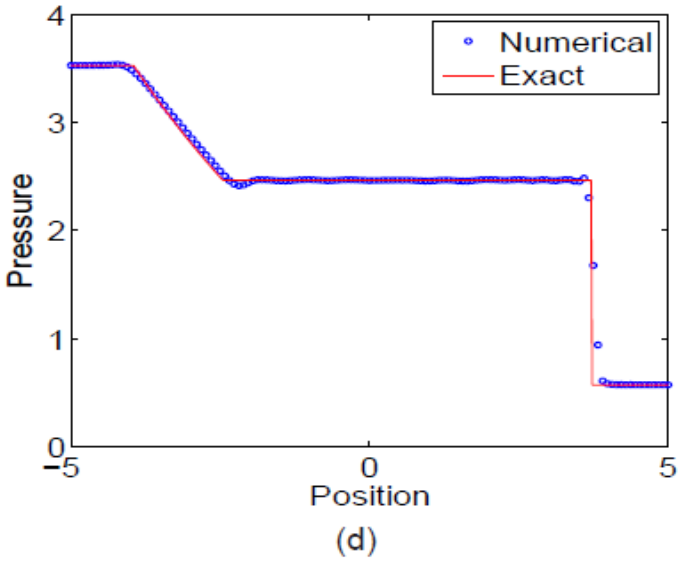

Figure 7: Comparison of numerical results from the 6th-order PDE transform and the FPM-RSK for Lax's problem ($t = 1.5$, $\Delta t = 0.02$, 129 grid points). (a) Density from the PDE transform; (b) Pressure from the PDE transform; (c) Density from the FPM-RSK; (d) Pressure from the FPM-RSK.

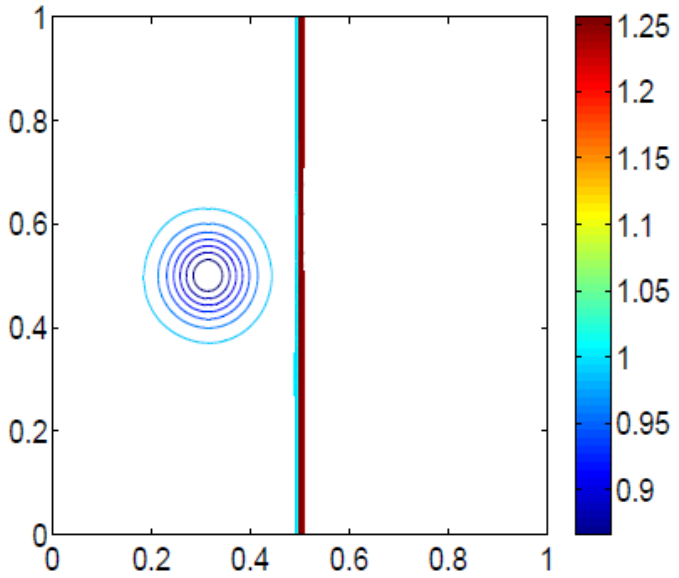

(a) $t = 0.05$

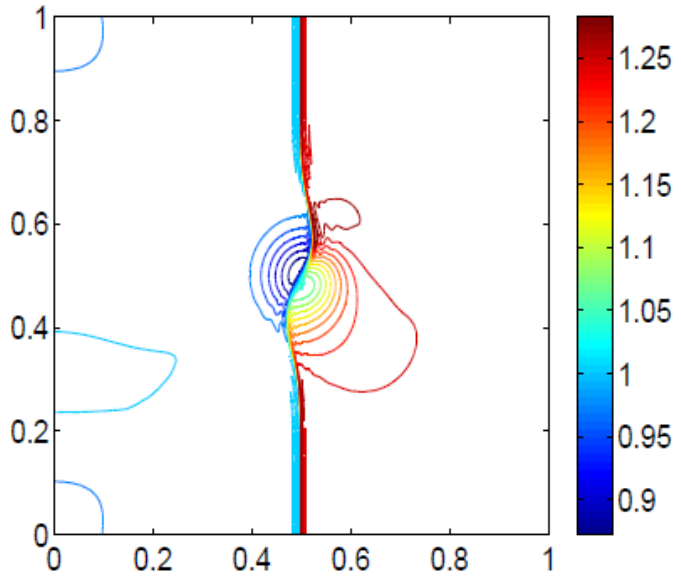

(b) $t = 0.2$

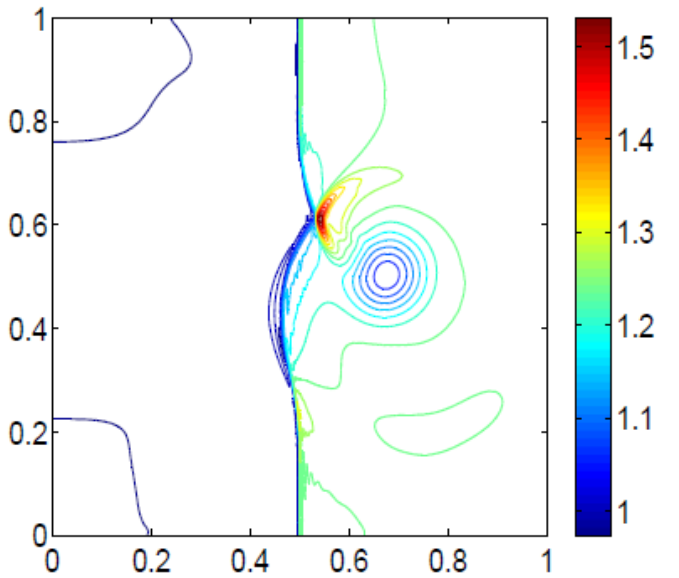

(c) $t = 0.35$

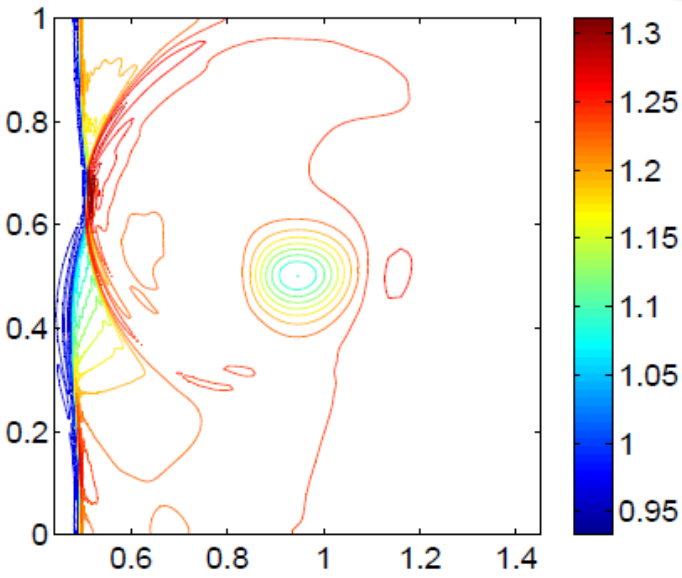

(d) $t = 0.6$

PDE transform for hyperbolic conservation laws

Figure 12: The pressure profile of 2D shock-vortex interaction problem from the 10th-order PDE transform (20 contours).

Comparison of Hilbert-Huang, wavelet, Fourier and PDE transforms

- Only yield the relevant functional modes
- Each mode contains desired frequency range
- Mode is extracted using accurate high order PDEs based band-pass filters

- Each sub-band width is totally controllable
- Each mode function is determined by PDE order and evolution time
- Adjustable dual temporal-frequency localization

- Each mode contains selected frequency range
- Physical domain representation
- Applicable for non-stationary signal, and no Gibbs oscillations

Partial Differential Equation Transform

Hilbert-Huang transform	Wavelet transform	Fourier transform
• Each mode is obtained by spline based lowpass filter • Instantaneous frequency is obtained for characterizing non-stationary data	• Dual time-scale analysi • Robust choice of the mother wavelet • Dilation and translation are used to capture the local characteristics	• Perfect localization in frequency space • Gibbs oscillations • Impressive improvements and applications are still occurring

Hierarchy of Methods

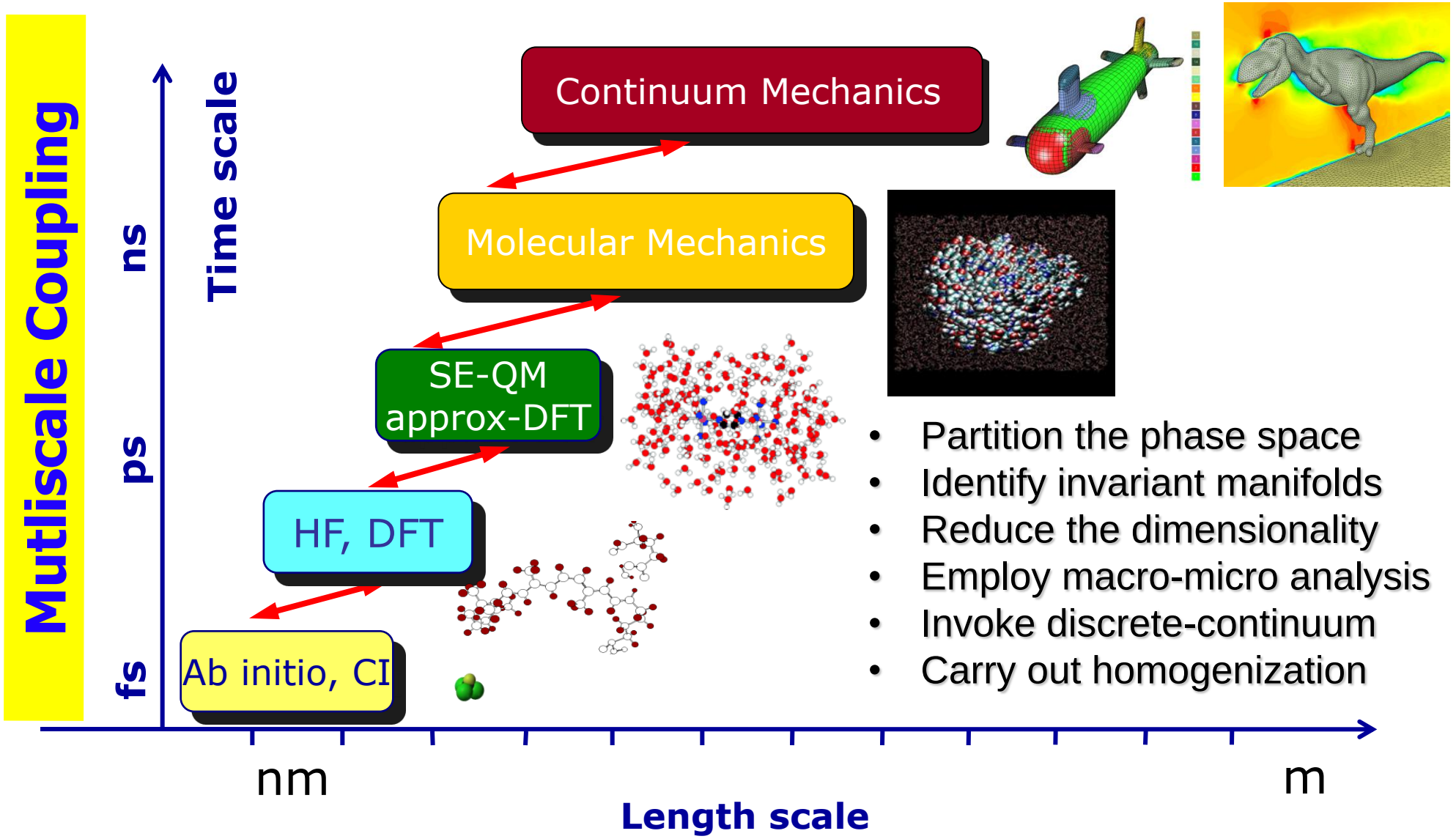

- Partition the phase space
- Identify invariant manifolds
- Reduce the dimensionality
- Employ macro-micro analysis
- Invoke discrete-continuum
- Carry out homogenization

Minimal Surfaces

A way to minimize energy and maximize stability

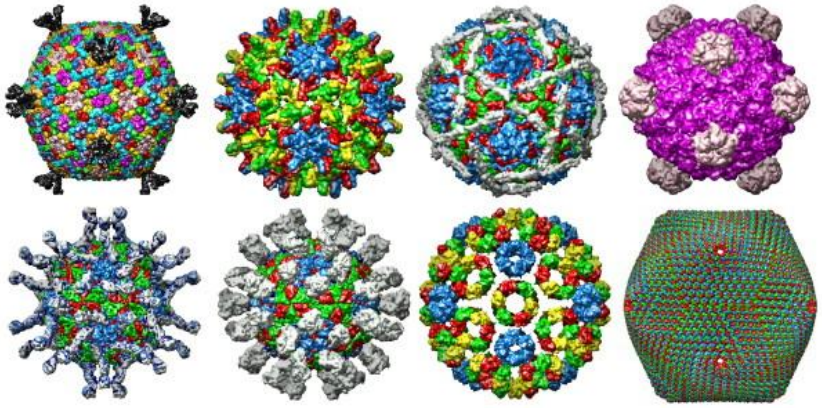

Viral morphology

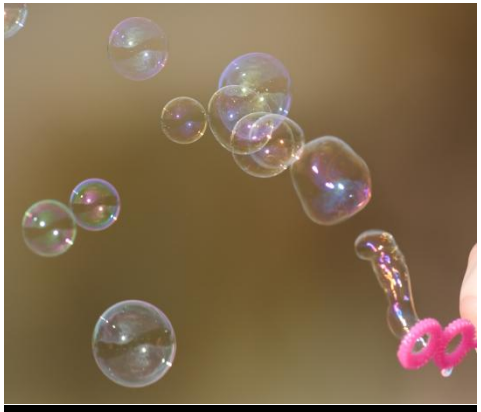

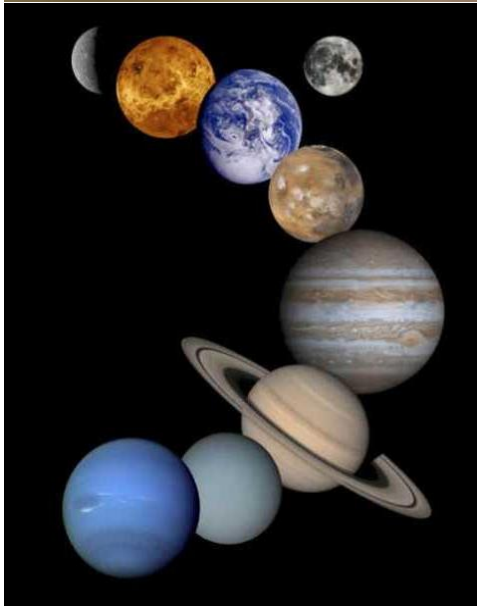

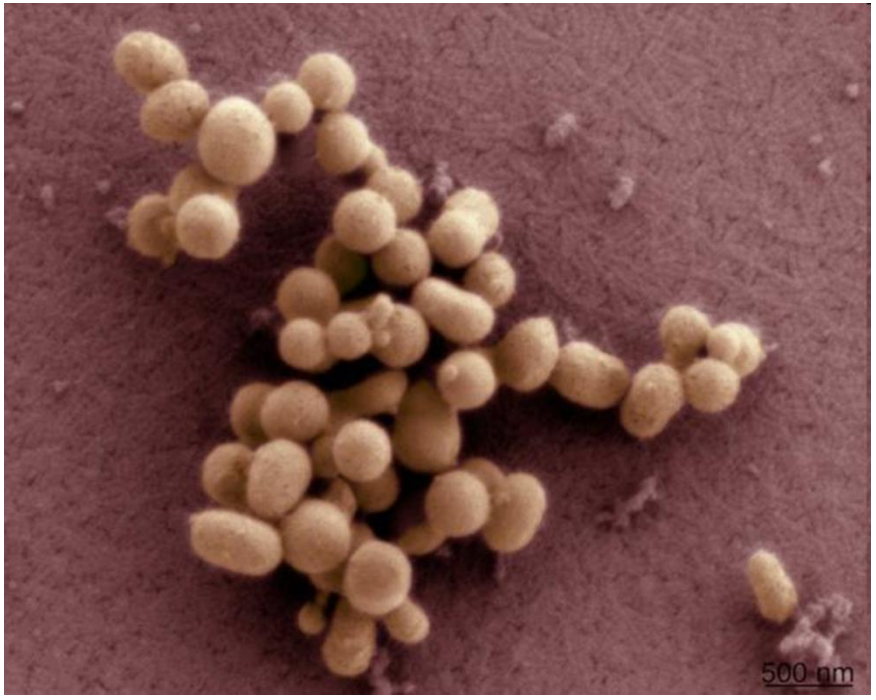

The first man-made life, Bacterium, *M. mycoides*, based on information from a computer

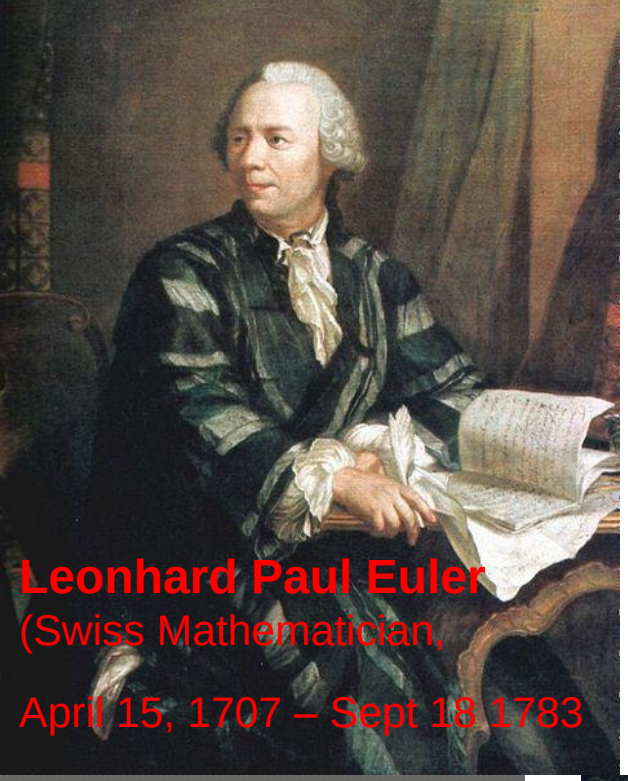

Leonhard Paul Euler
(Swiss Mathematician,
April 15, 1707 – Sept 18 1783

Catenoid

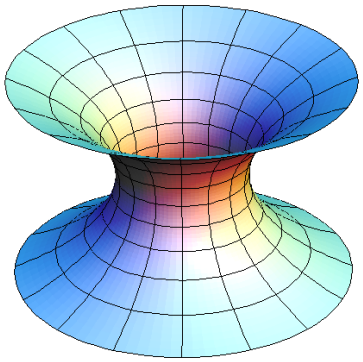

Minimal Surfaces

Joseph-Louis Lagrange
(Italian Mathematician,
January 25 1736 – April 10, 1813)

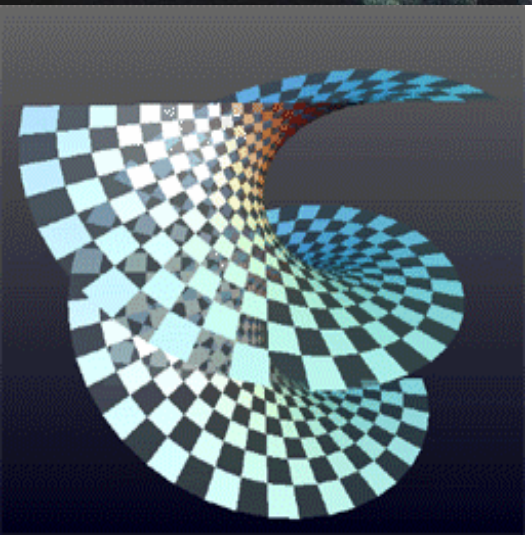

Helicoid

Jean Baptiste Meusnier
(French, June 19, 1754-June 13, 1793)

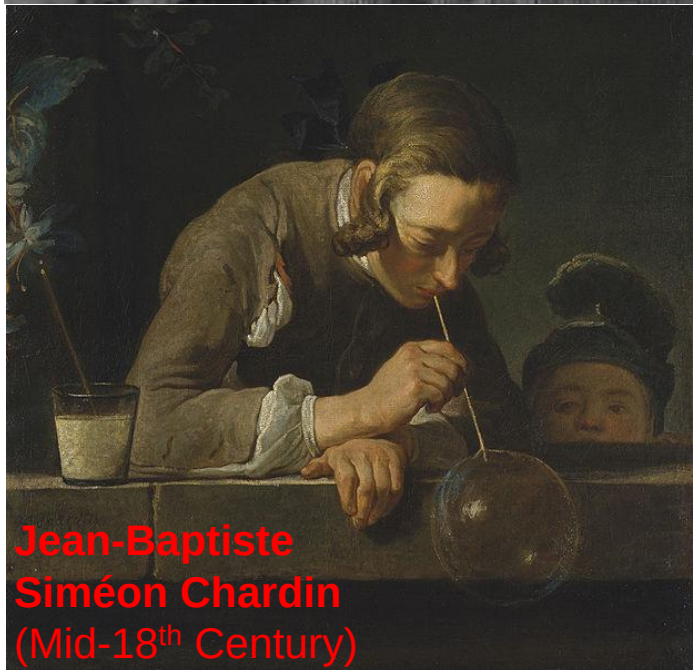

Jean-Baptiste Siméon Chardin
(Mid-18th Century)

Geometric flow based minimal surface model

$$G = \int_{\Omega} [area] dr$$

(Bates, Wei, Zhao, JCC,2008)

$$area = \gamma |\nabla S|$$

where gamma (γ) is the surface tension, and S is a characteristic function:

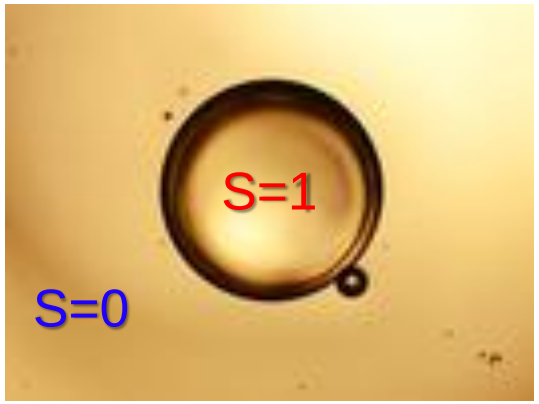

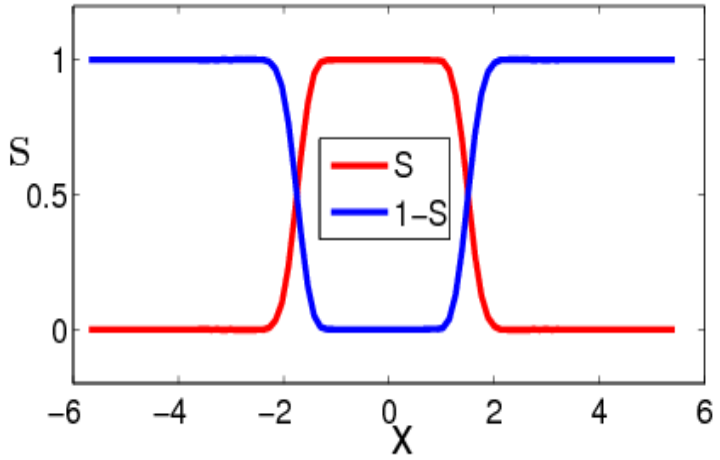

Generalized Laplace-Beltrami flow (Mean curvature flow):

$$\frac{\partial S}{\partial t} = |\nabla S| \left[\nabla \bullet \frac{\gamma \nabla S}{|\nabla S|} \right]$$

Minimal Molecular surface

The first biomolecular surface constructed with the variational principle

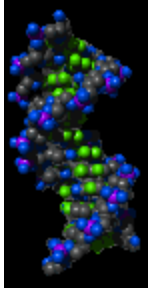

Generalized Laplace-Beltrami flow:

$$\frac{\partial S}{\partial t} = |\nabla S| \left[\nabla \bullet \frac{\gamma \nabla S}{|\nabla S|} \right]$$

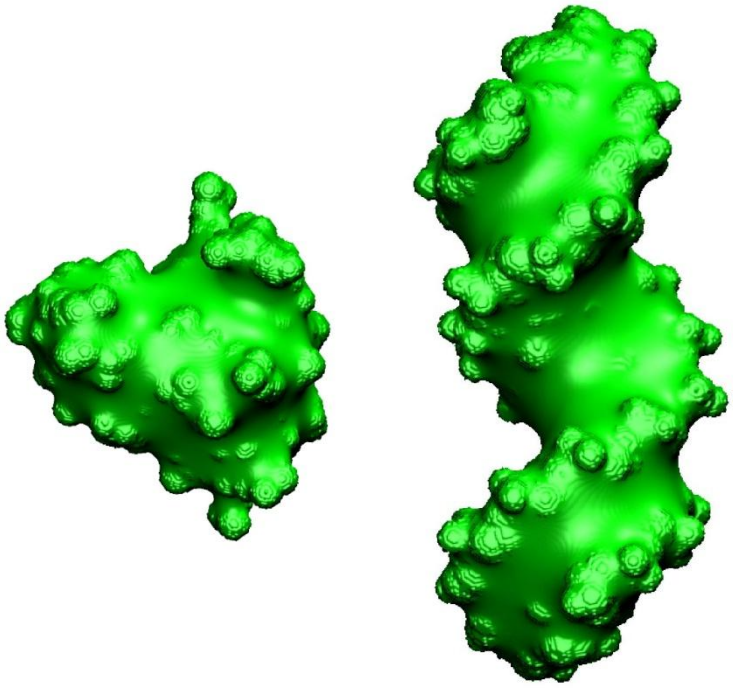

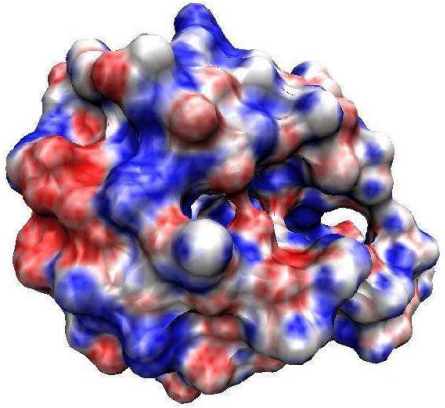

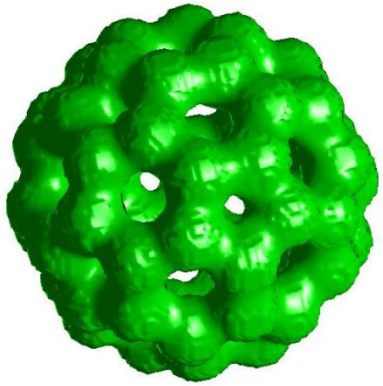

Bates, Wei & Zhao, 2006
J. Comput. Chem. 2008

Virus surfaces

1CGM

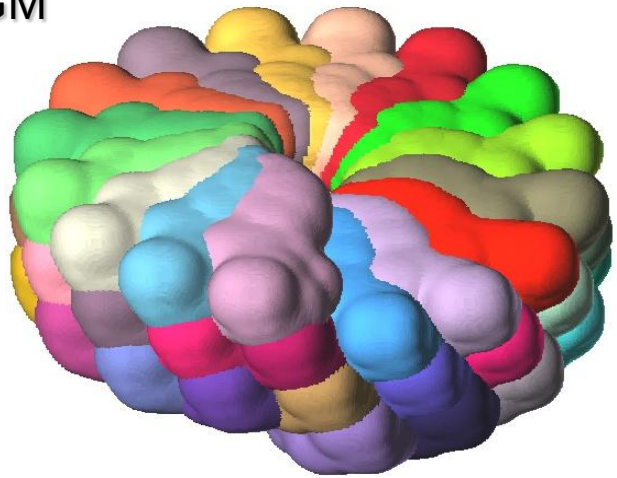

1EI7

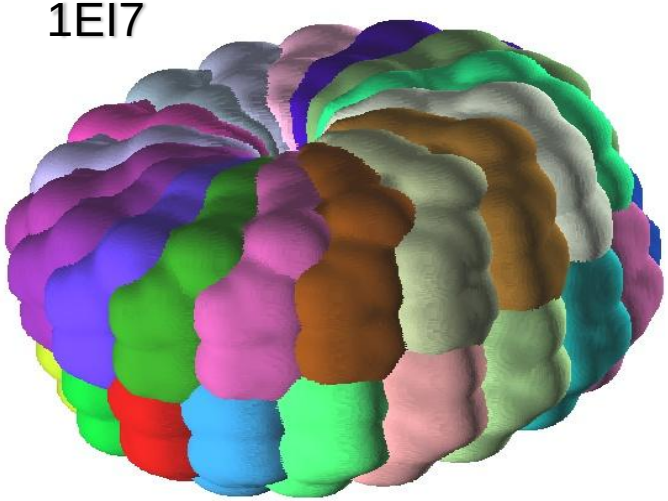

1NOV

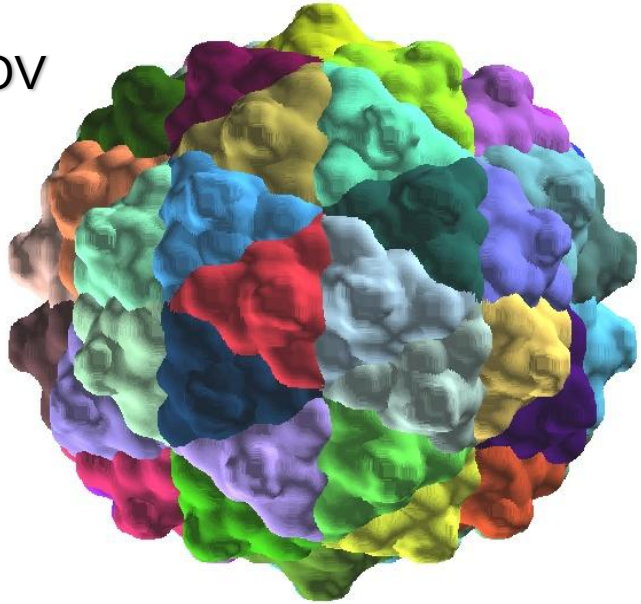

2BK1

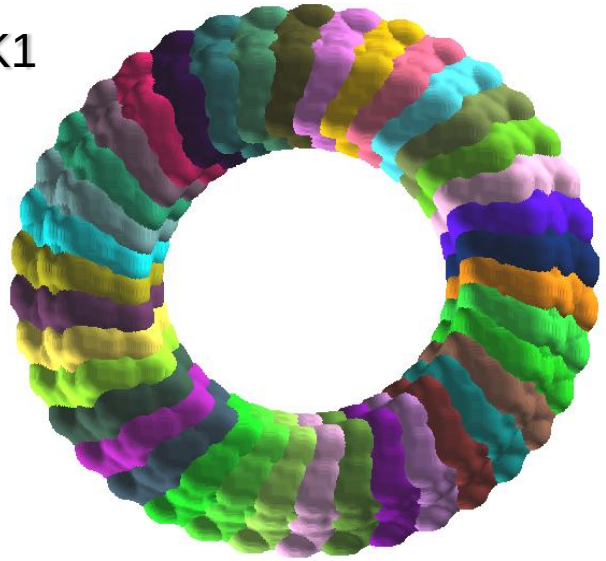

Chen, Saxena, Wei, IJBI, 2009

Solvation analysis

Physiological fact: 65-90% cell mass is water

Protein in vacuum:

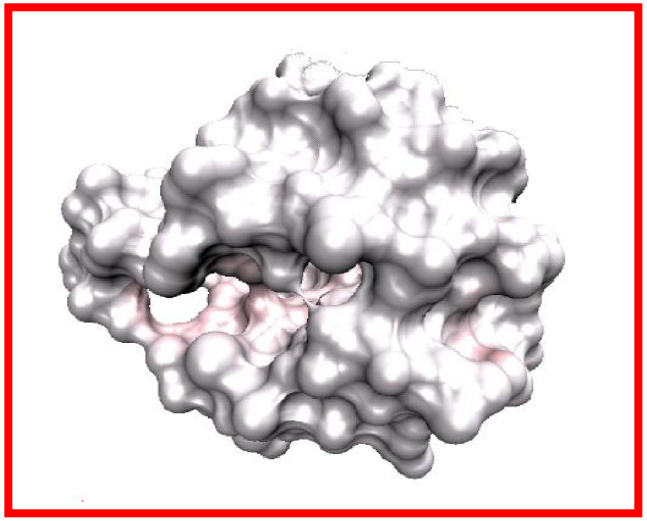

Protein in water:

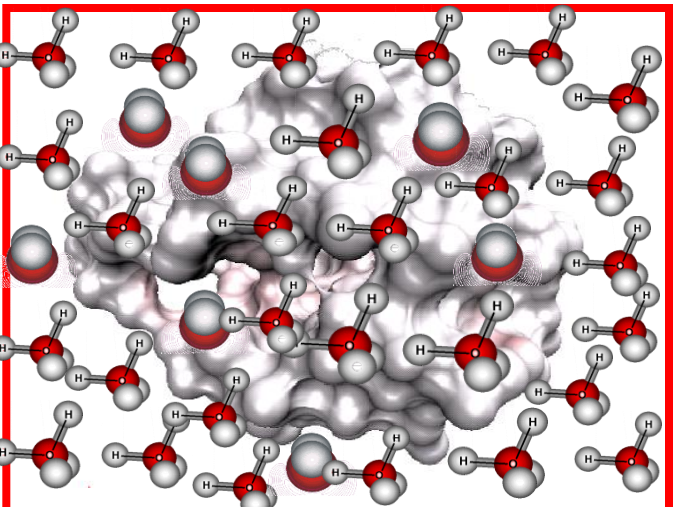

Solvation

Implicit solvent model

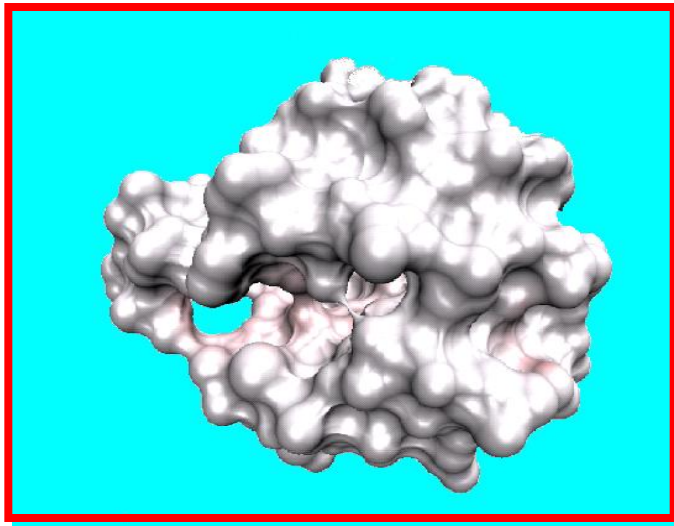

Differential geometry based nonpolar solvation model

$$G = \int_{\Omega} \left[\gamma |\nabla S| + Sp + (1-S)U \right] dr$$

(Wei, BMB, 2010;
Chen, Zhao, Baker, Bates, Wei, 2011)

area + volume + van der Waals

$$\frac{\partial S}{\partial t} = |\nabla S| \left[\nabla \bullet \frac{\gamma \nabla S}{|\nabla S|} - p + U \right]$$

Laplace-Beltrami equation

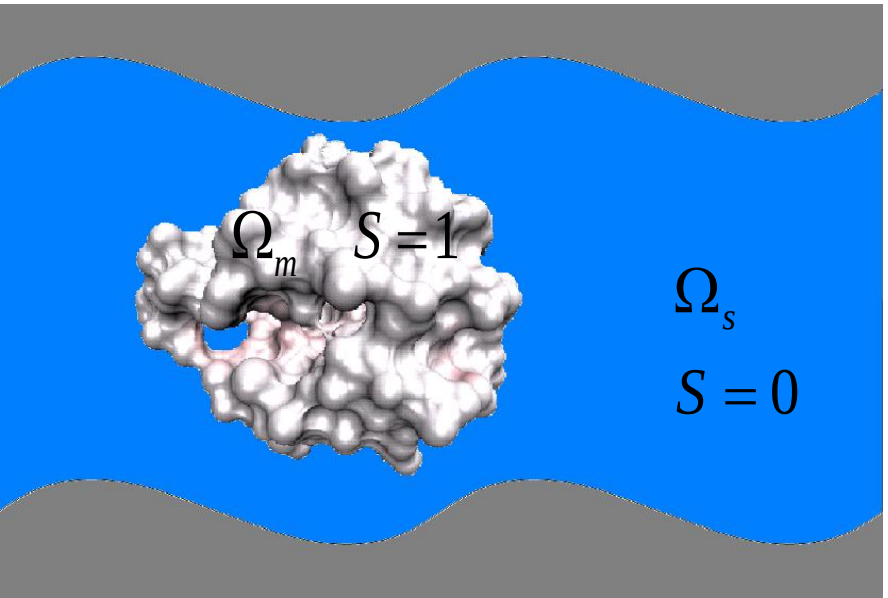

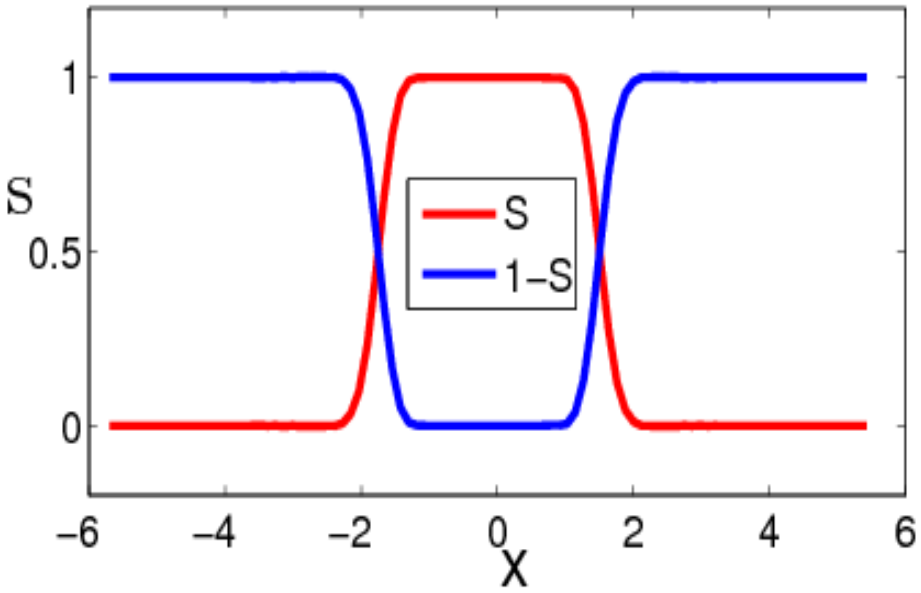

Comparison of nonpolar solvation free energies

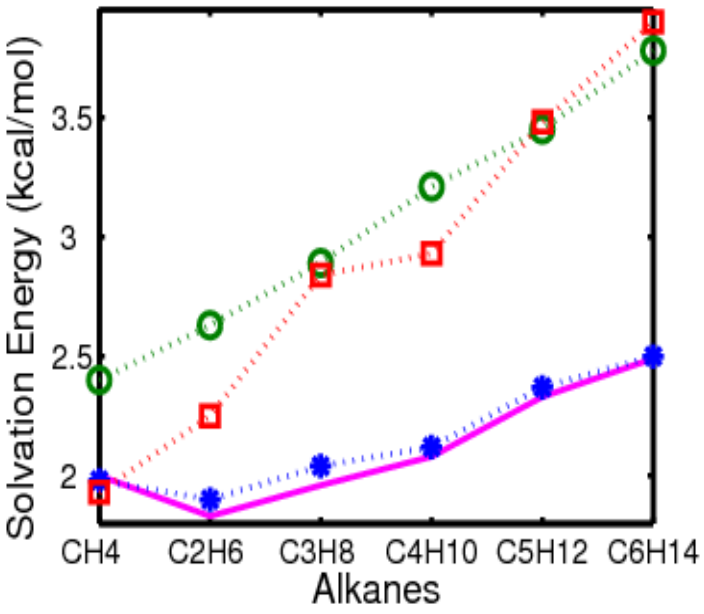

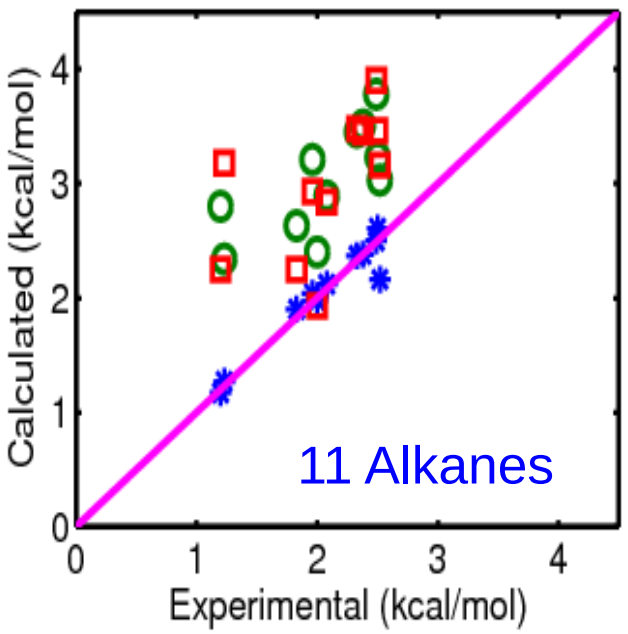

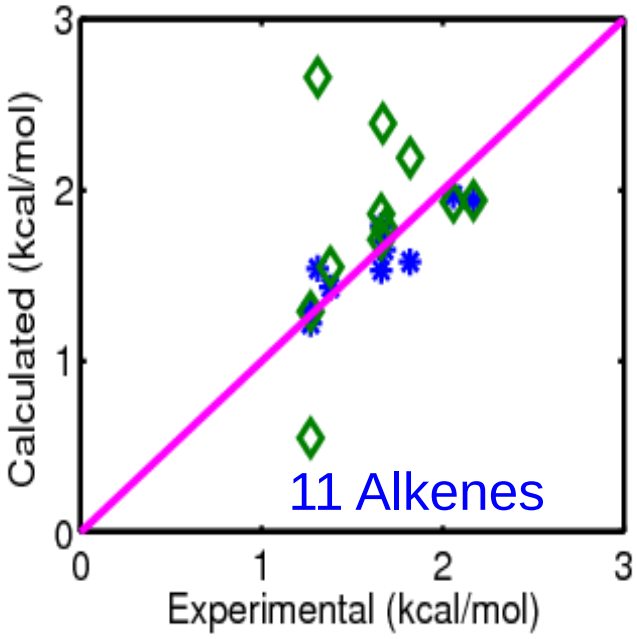

- Variational multiscale (Chen, Zhao, Baker, Bates, Wei, 2011)
- Wagoner and Baker. PNAS,103, 8331, 2006.
- Gallicchio, Kubo, Levy, J. Phys. Chem. B, 104, 6271, 2000
- Ratkova et al, (integral eqn theory) J. Phys. Chem. B, 114, 12068, 2010.

Differential geometry based solvation model

$$G = \int_{\Omega} [Nonpolar + Electro]\, dr$$

(Wei, BMB, 2010;
Chen, Baker, Wei, JCP,2010)

Geometric = area + volume + van der Waals:

$$Nonpolar = \gamma |\nabla S| + Sp + (1 - S)U$$

Electro = electric field + solute charges + solvent ions:

$$Electro = S\left(\frac{\varepsilon_m}{2}|\nabla\phi|^2 - \phi n\right) + (1-S)\left[\frac{\varepsilon_s}{2}|\nabla\phi|^2 + kT\sum_i c_i\left(e^{-q_i\phi/kT} - 1\right)\right]$$

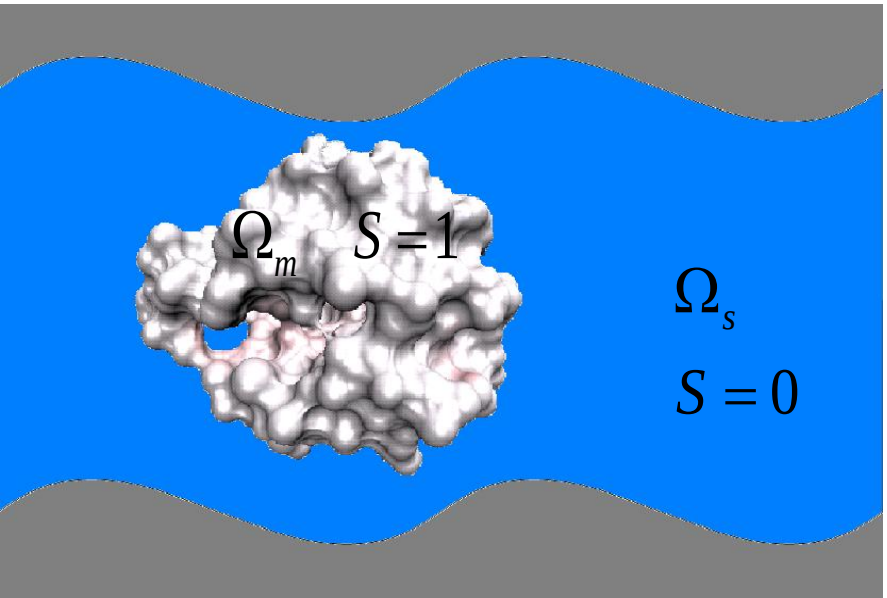

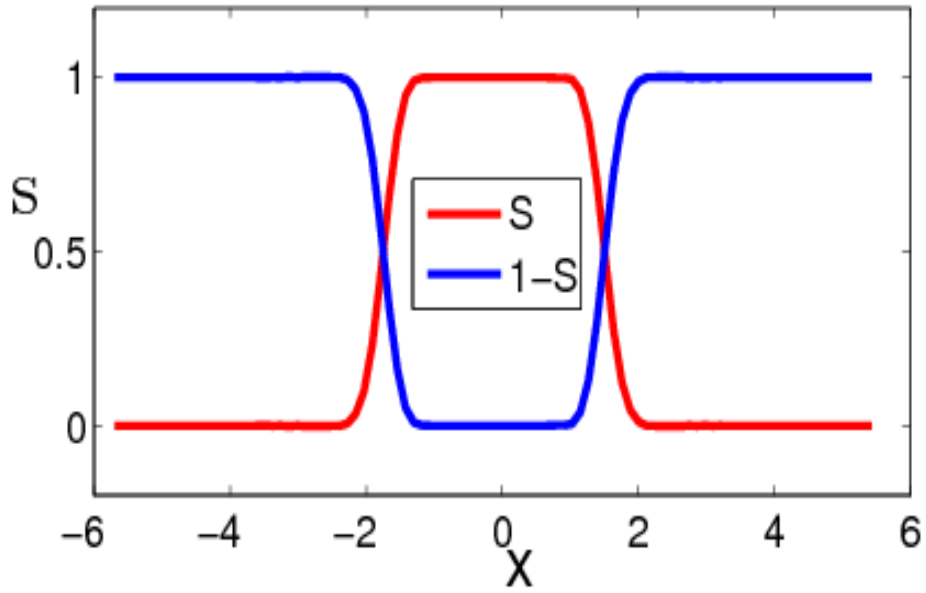

Variation of the total free energy functional

$$\frac{\partial S}{\partial t} = \nabla \bullet \left(\gamma \frac{\nabla S}{|\nabla S|} \right) - p + U - \frac{\varepsilon_m - \varepsilon_s}{2} |\nabla \phi|^2 + kT \sum_i c_i \left(e^{-q_i \phi / kT} - 1 \right) - \phi n$$

Generalized Laplace Beltrami equation

$$-\nabla \bullet \left(\varepsilon(S) \nabla \phi \right) = (1 - S) \sum_i q_i c_i e^{-q_i \phi / kT} + Sn$$

Generalized Poisson-Boltzmann equation

Applications

- Electrostatic binding and solvation energies
- pKa, pH values
- Electrostatic forces, ionic distributions
- Electrostatic matching between proteins and ligands
- Stability of protein folding
- Molecular dynamics
- A tool for rational drug design (interactions of receptor-inhibitor, protein-ligand, protein-protein, signal, enzyme, regulator, etc.)

Validation of the multiscale solvation model

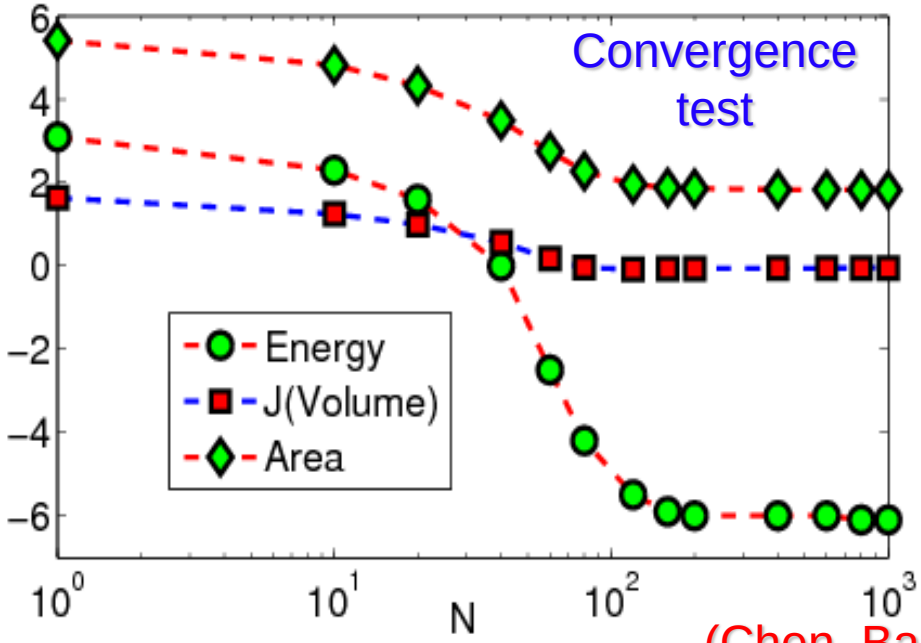

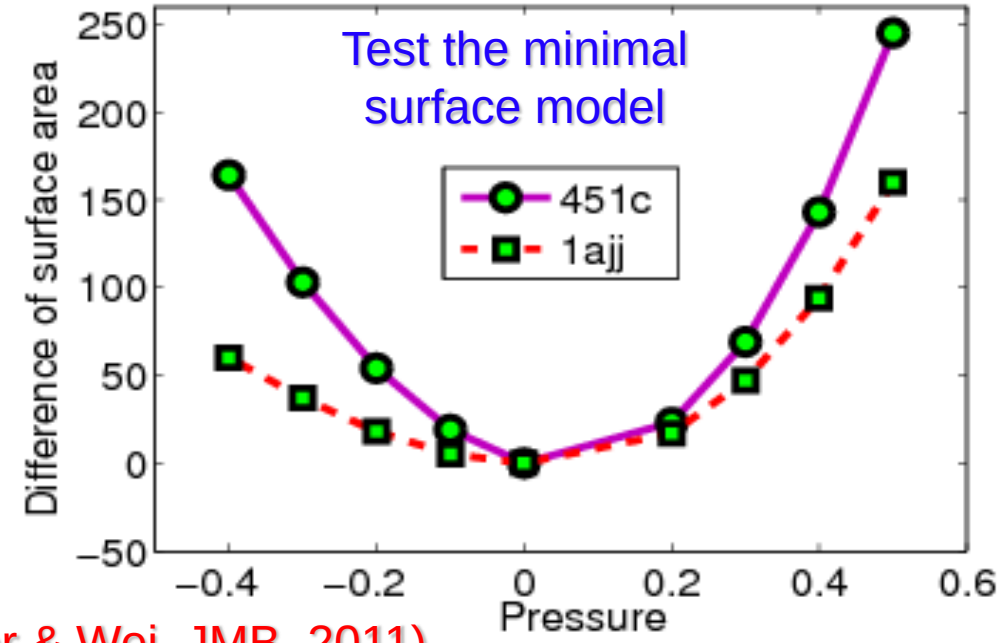

(Chen, Baker & Wei, JMB, 2011)

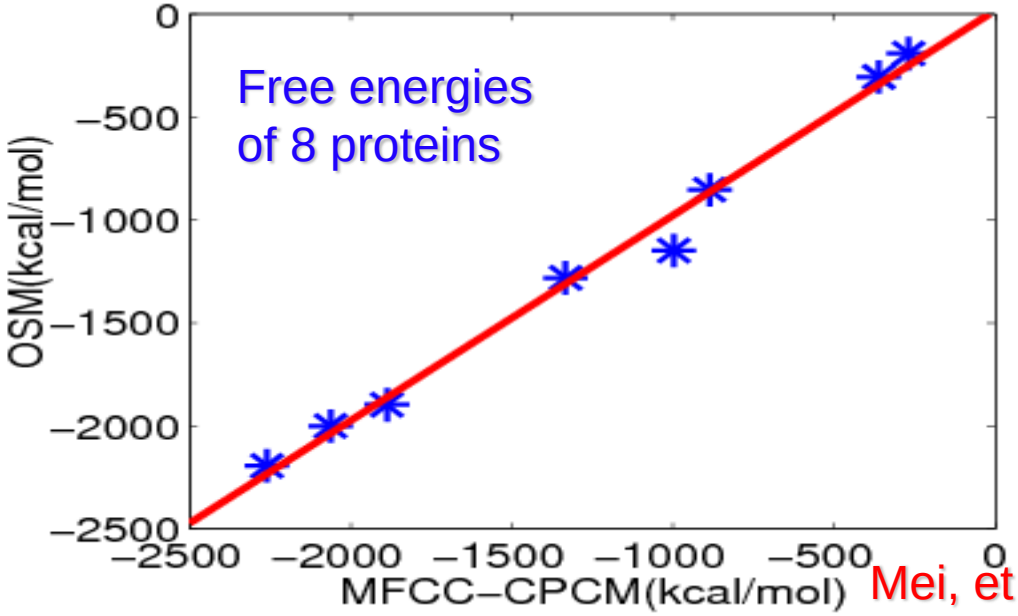

Mei, et al, 2006

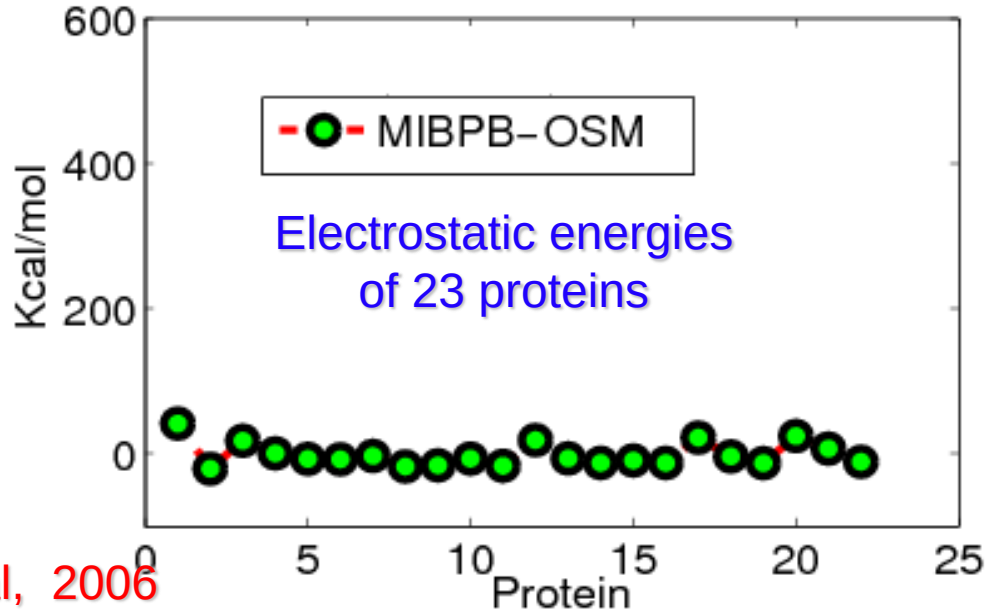

Effect of interaction potentials

(Chen, Baker & Wei, JCP, 2010)

$$\frac{\partial S}{\partial t} = \sqrt{g}\left[\nabla \cdot \left(\frac{\nabla S}{\sqrt{g}}\right) - V\right]$$

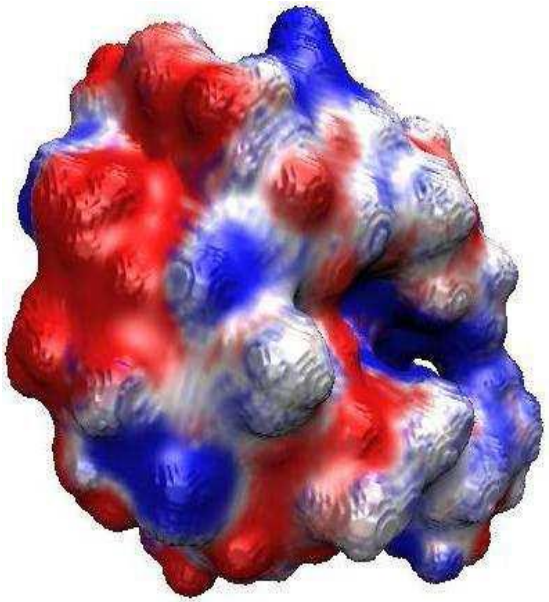

Minimal molecular surface

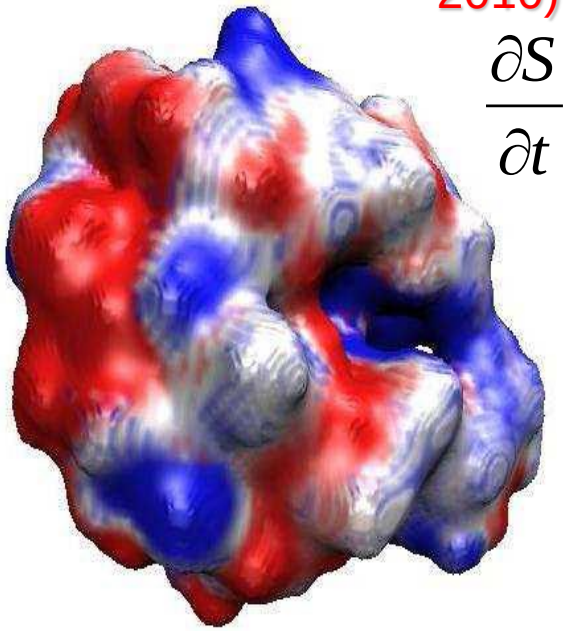

Repulsive surface

Protein 451c

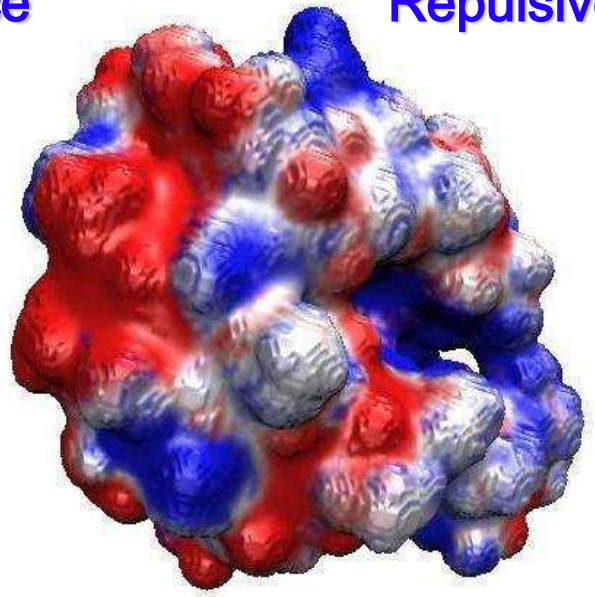

Attractive surface

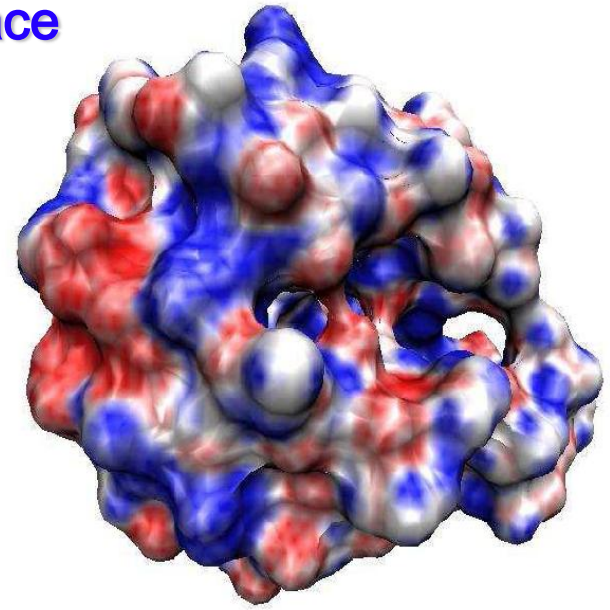

Connolly surface

Blind test of 17 compounds: No parameter fitting! (Chen, Baker & Wei, JCP, 2010)

Compound	Area	Volume	G_{np}	ΔG_p	ΔG	Exptl	Error
glycerol triacetate	241.34	234.11	2.33	-12.36	-10.03	-8.84	-1.19
benzyl bromide	150.66	136.36	1.39	-4.87	-3.47	-2.38	-1.09
benzyl chloride	148.14	133.84	1.36	-5.06	-3.70	-1.93	-1.77
m-bis(trifluoromethyl)benzene	266.67	306.86	2.22	-3.30	-1.07	1.07	-2.14
N,N-dimethyl-p-methoxybenzamide	209.31	202.02	1.99	-9.22	-7.22	-11.01	3.79
N,N-4-trimethylbenzamide	200.27	193.25	1.91	-7.84	-5.93	-9.76	3.83
bis-2-chloroethyl ether	155.71	130.90	1.44	-4.16	-2.71	-4.23	1.52
1,1-diacetoxyethane	177.82	160.48	1.67	-8.21	-6.53	-4.97	-1.56
1,1-diethoxyethane	163.66	143.73	1.55	-4.63	-3.08	-3.28	0.20
1,4-dioxane	109.56	143.73	1.01	-5.64	-4.62	-5.05	0.43
diethyl propanedioate	195.06	182.22	1.87	-7.75	-5.88	-6.00	0.12
dimethoxymethane	109.17	88.36	1.02	-4.64	-3.62	-2.93	-0.69
ethylene glycol diacetate	168.19	160.95	1.62	-8.40	-6.78	-6.34	0.44
1,2-diethoxyethane	169.25	141.92	1.57	-4.40	-2.83	-3.54	0.71
diethyl sulfide	133.81	116.84	1.22	-2.40	-1.17	-1.43	0.26
phenyl formate	148.14	134.84	1.37	-7.82	-6.45	-4.08	-2.37
imidazole	89.05	68.59	0.80	-11.56	-10.76	-9.81	-0.95

RMS=1.78 compared with RMS=1.87 by Nicholls et al (2008)

Binding free energies of protein-protein interactions

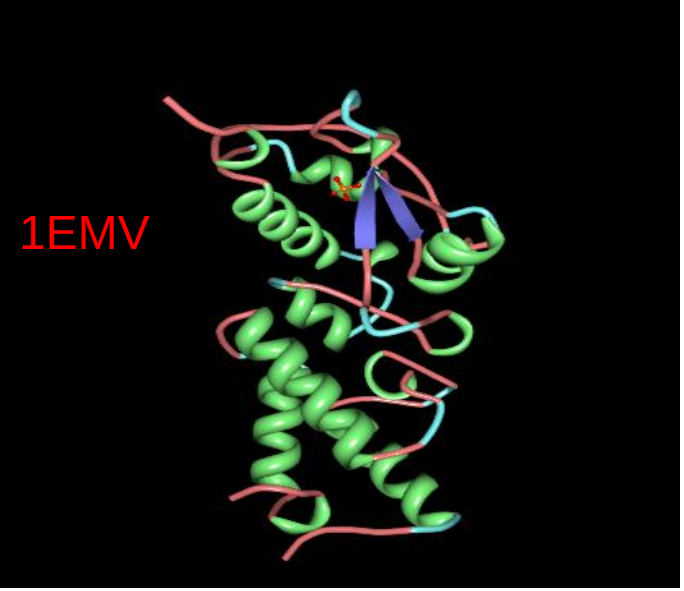

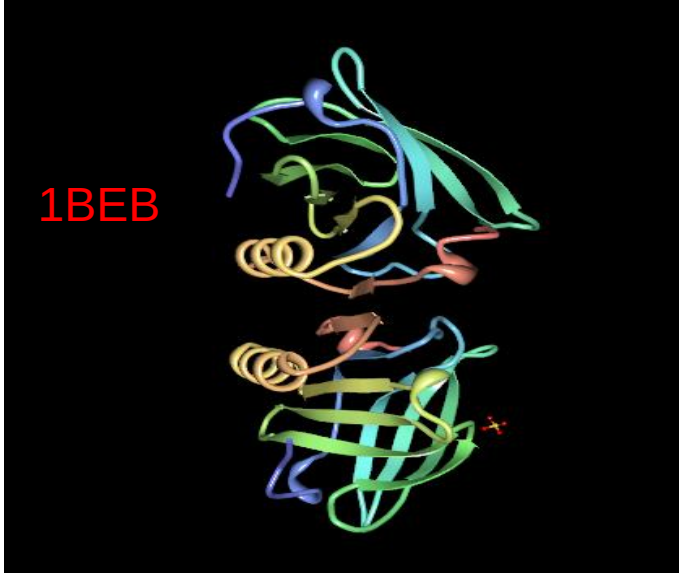

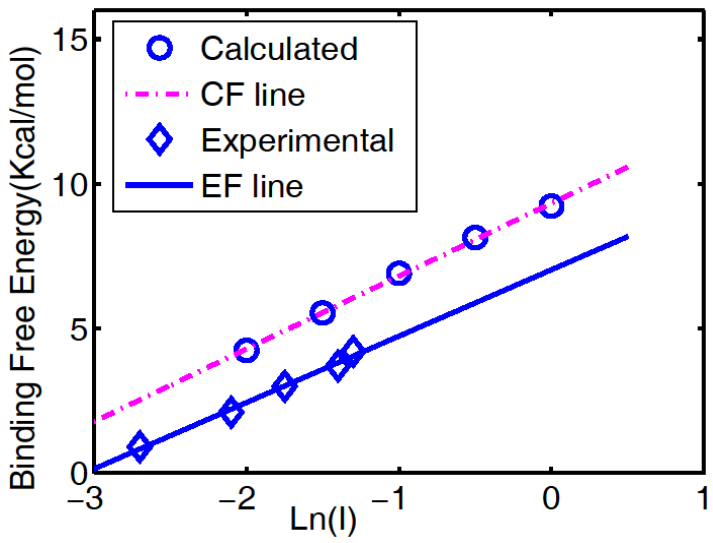

(Chen, Baker & Wei, JMB, 2011)

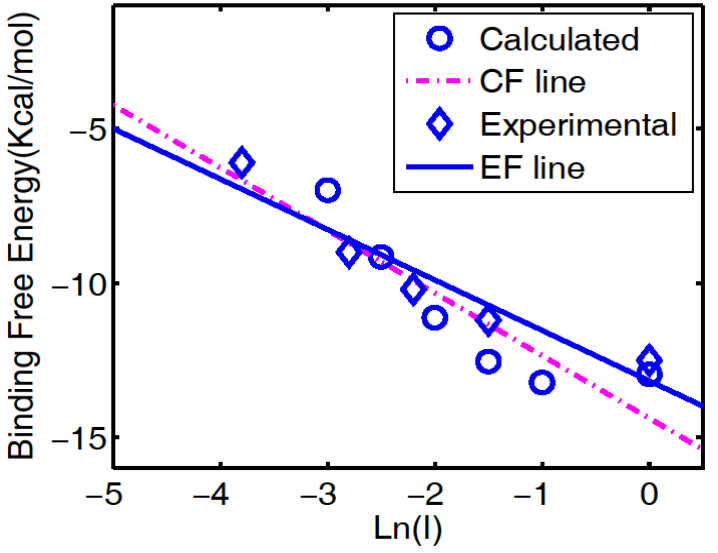

Complex	PDB code	Complex charge	Surface Area (Å²)	Charge of the free monomers	Experimental data	Calculated
E9Dnase-Im9 (10)	1emv	-3	1465	B=+5; A=-8	2.17	2.52
Lactoglobulin Dimer (57) (A-B)	1beb	+26	1167	A=B=+13	-1.62	-2.02

Acid-Sensing Ion Channel in Inflammatory Pain Hypersensitivity

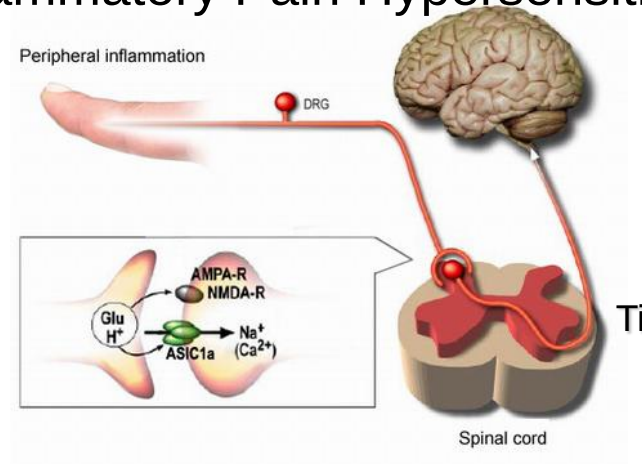

Tian-Le Xu

Increased ASIC ion channel activity in SDH neurons promotes pain by central sensitization

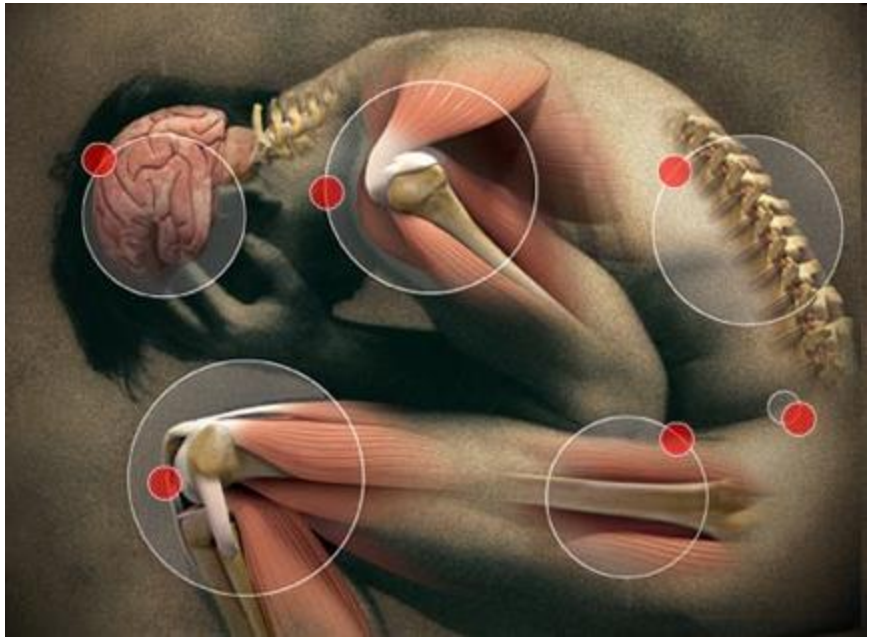

The molecular mechanisms of inherited arrhythmia

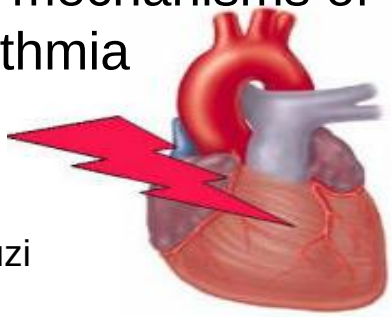

M. Tristani-Firouzi

Mutations in K^+ channel cause a decreased outward K^+ current during the plateau phase of the cardiac action potential, and lead to cardiac arrhythmias and sudden death

How Human Ear Translates Vibrations Into Sounds: Discovery Of Ion Channel Turns Ear On Its Head

Anthony Ricci

Inner hair cell mechanotransducer calcium channels turns sounds into electrical current

Physiological Facts

Human beings (and other living organisms) are run by electricity, and ion channels are the core of our electrical system.

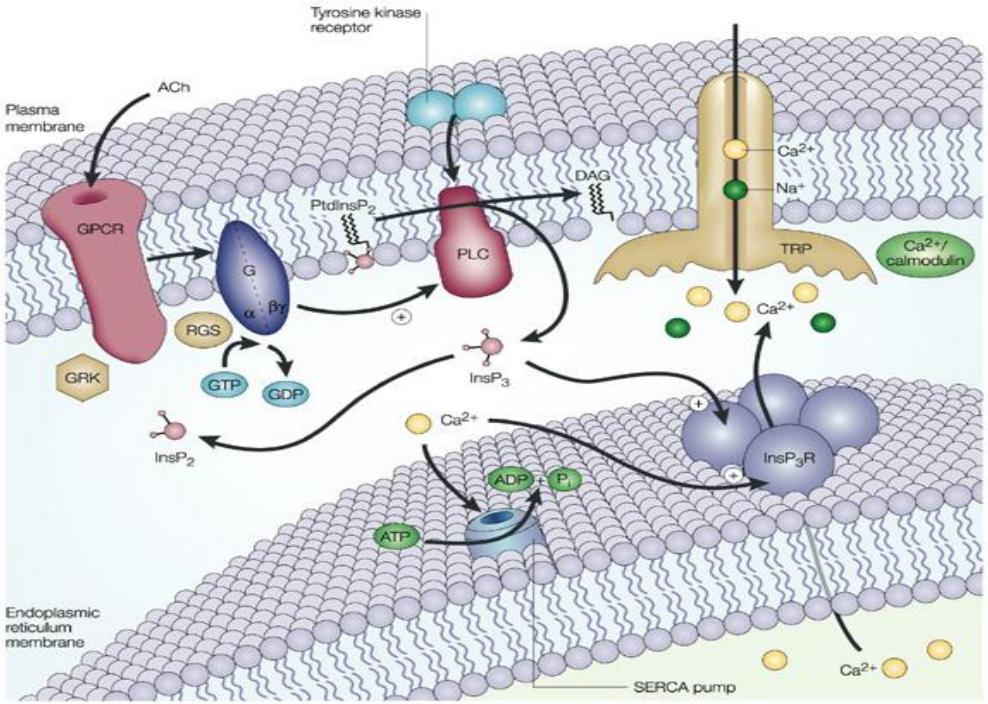

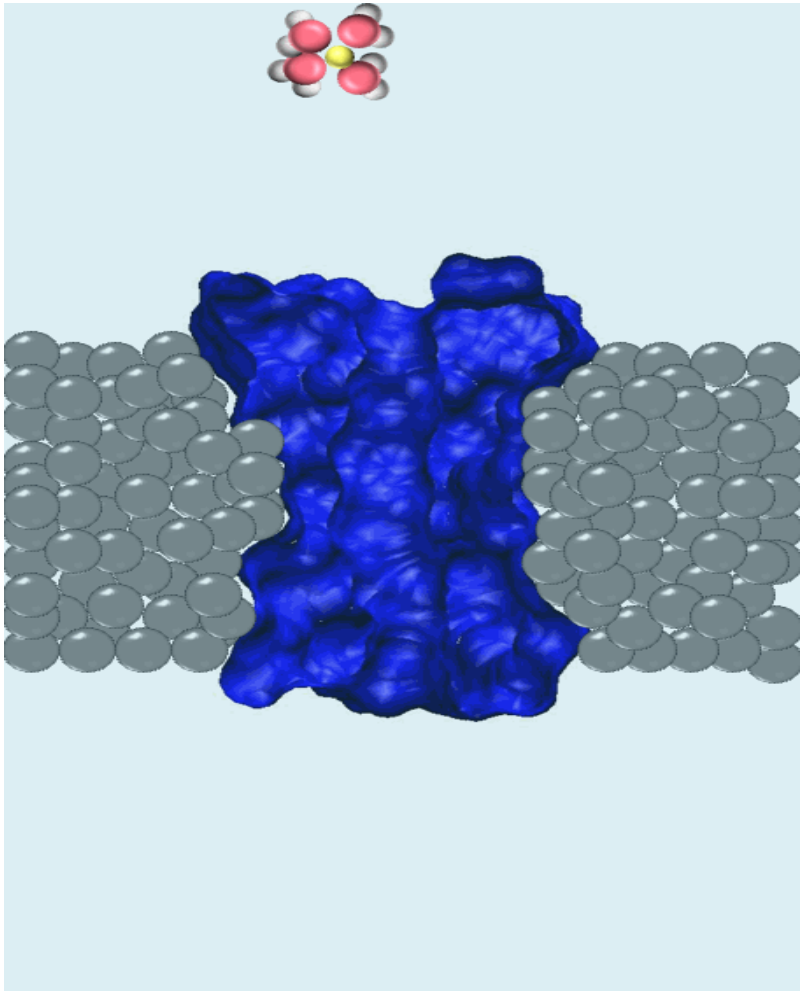

- Ion channels are small highly selective pores in the cell membrane
- Move ions or water
- Fast rate of transport 10^6 ions/s
- Transport is always down the gradient
- Non-equilibrium process

Differential geometry based Poisson-Nernst-Planck

(Zheng, Chen, & Wei, 2011)

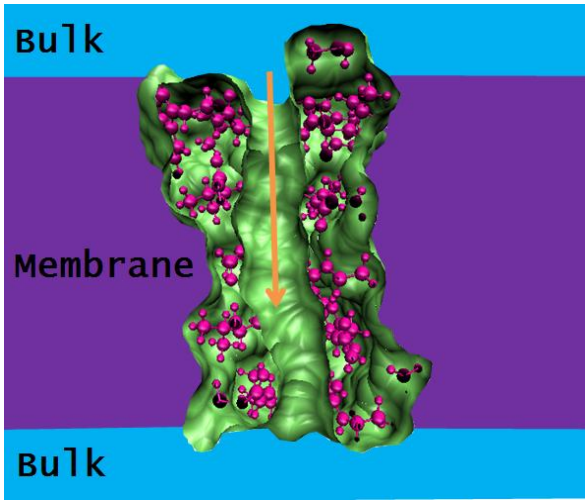

$$G = \int \{Nonpolar + Electro + Chemical\} dx$$

$$G_{Nonpolar} = \gamma |\nabla S| + Sp + (1-S)\sum_{\alpha} n_\alpha U_\alpha$$

$$G_{Electro} = S\left[\phi \sum_j Q_j \delta(r - r_j) - \frac{\varepsilon_m}{2}|\nabla \phi|^2\right] + (1-S)\left[\sum_\alpha n_\alpha q_\alpha \phi - \frac{\varepsilon_s}{2}|\nabla \phi|^2\right]$$

$$G_{Chemical} = (1-S)\sum_\alpha n_\alpha \left[\mu_{0\alpha} + kT\left(\ln \frac{n_\alpha}{n_{\alpha 0}} - 1\right)\right]$$

Nonpolar: Surface energy, mechanical work and general interactions
Electro: Electrostatic energies in protein and in solvent
Chemical: Chemical potentials and concentration effect

Generalized Poisson equation

$$\frac{\delta G}{\delta \phi} \Rightarrow -\nabla \bullet \varepsilon(S)\nabla\phi = S\sum_j Q_j \delta(r - r_j) + (1-S)\sum q_\alpha n_\alpha$$

$$\varepsilon(S) = S\varepsilon_m + (1-S)\varepsilon_s$$

Electrochemical potential

$$\frac{\delta G}{\delta n_\alpha} \Rightarrow \mu_\alpha = \mu_{0\alpha} + kT \ln \frac{n_\alpha}{n_{\alpha 0}} + q_\alpha \phi + U_\alpha$$

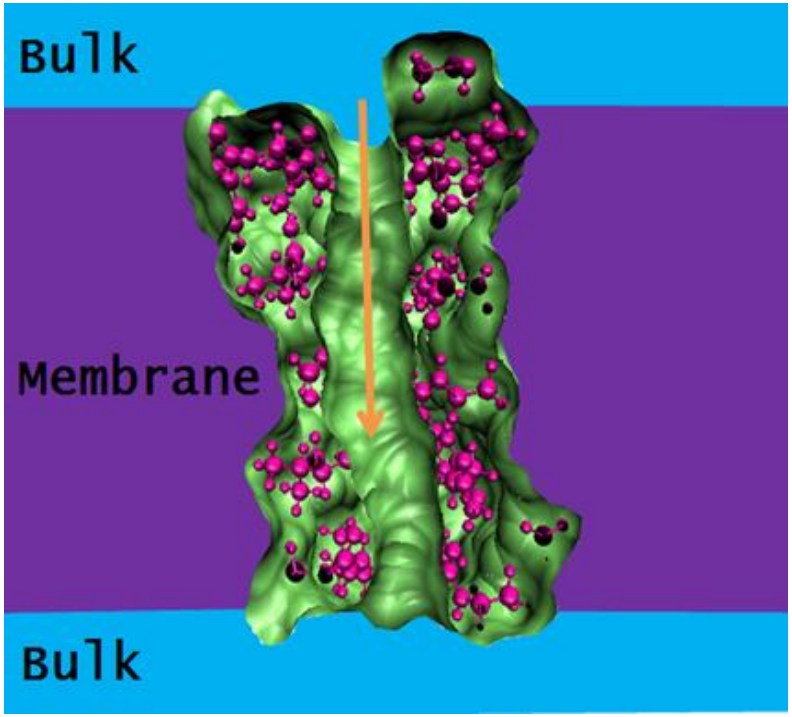

Nernst-Planck equation

$$J_\alpha = -D_\alpha n_\alpha \nabla \frac{\mu_\alpha}{kT}, \qquad \frac{\partial n_\alpha}{\partial t} = -\nabla \bullet J_\alpha$$

$$\frac{\partial n_\alpha}{\partial t} = \nabla \bullet \left[D_\alpha \left(\nabla n_\alpha + \frac{q_\alpha n_\alpha}{kT} \nabla [\phi + U_\alpha] \right) \right]$$

Generalized Laplace-Beltrami equation

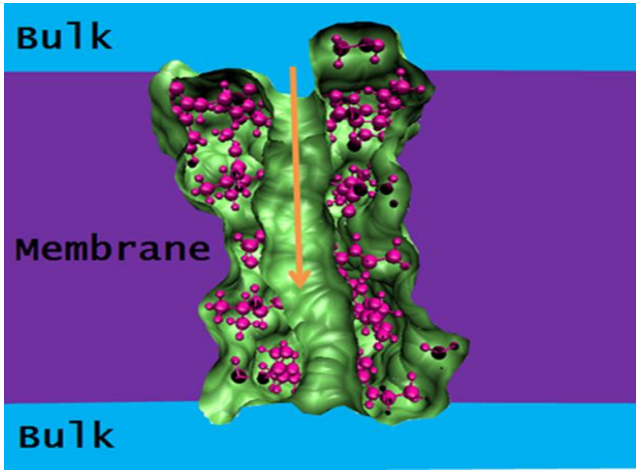

$$\frac{\delta G}{\delta S} \Rightarrow$$

$$\frac{\partial S}{\partial t} = |\nabla S| \left[\nabla \bullet \frac{\gamma \nabla S}{|\nabla S|} + V_{LB} \right]$$

$$V_{LB} = -p + \sum_{\alpha} n_{\alpha} U_{\alpha}$$

$$-\phi \sum_{j} Q_j \delta(r - r_j) + \frac{\varepsilon_m}{2} |\nabla \phi|^2 + \sum_{\alpha} n_{\alpha} q_{\alpha} \phi - \frac{\varepsilon_s}{2} |\nabla \phi|^2$$

$$+ \sum_{\alpha} n_{\alpha} \left[\mu_{0\alpha} + kT \left(\ln \frac{n_{\alpha}}{n_{\alpha 0}} - 1 \right) \right]$$

Computational issues

Channel surface

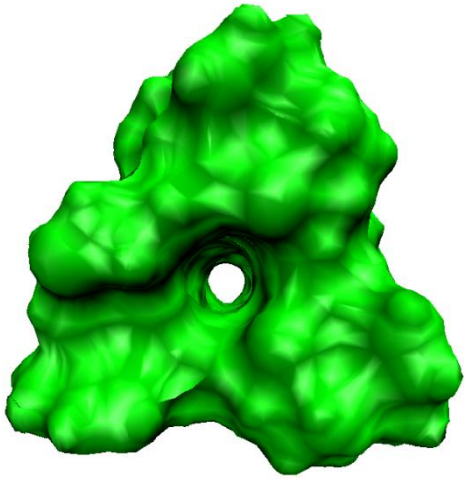

Computational domain

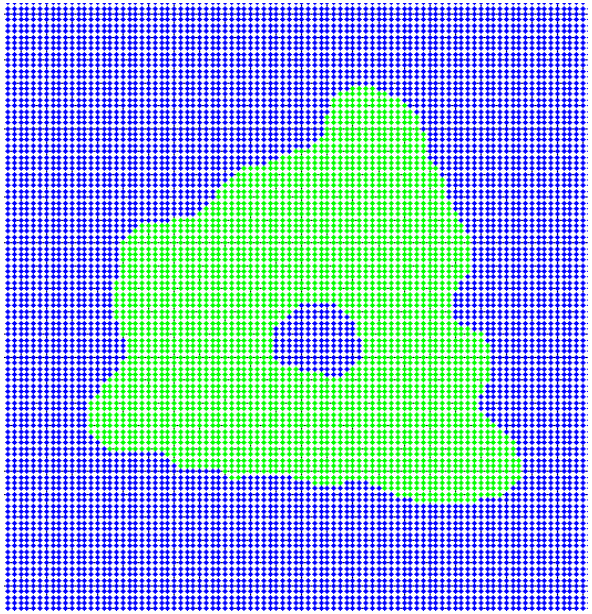

Electrostatic potential

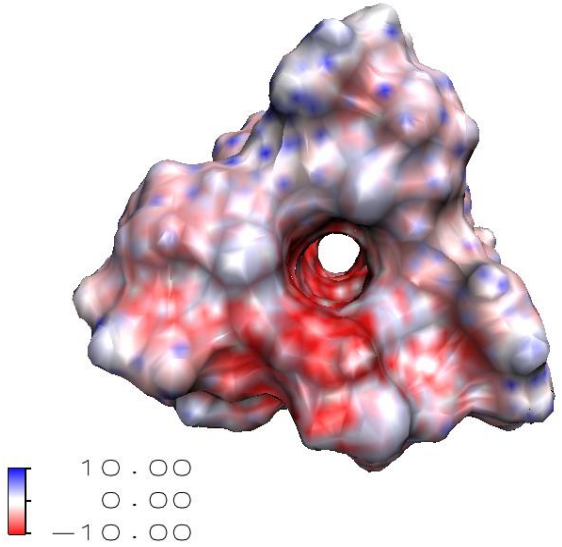

Boundary conditions:

Poisson equation: Dirichlet and Neumann

Nernst-Planck equation: Non-flux at the interface and Dirichlet

Laplace-Beltrami equation: Dirichlet

Numerical methods

Matched interface and boundary (MIB, 2nd order method!!!!)

Dirichlet to Neumann Mapping

Gummel iterations

Model validation at equilibrium

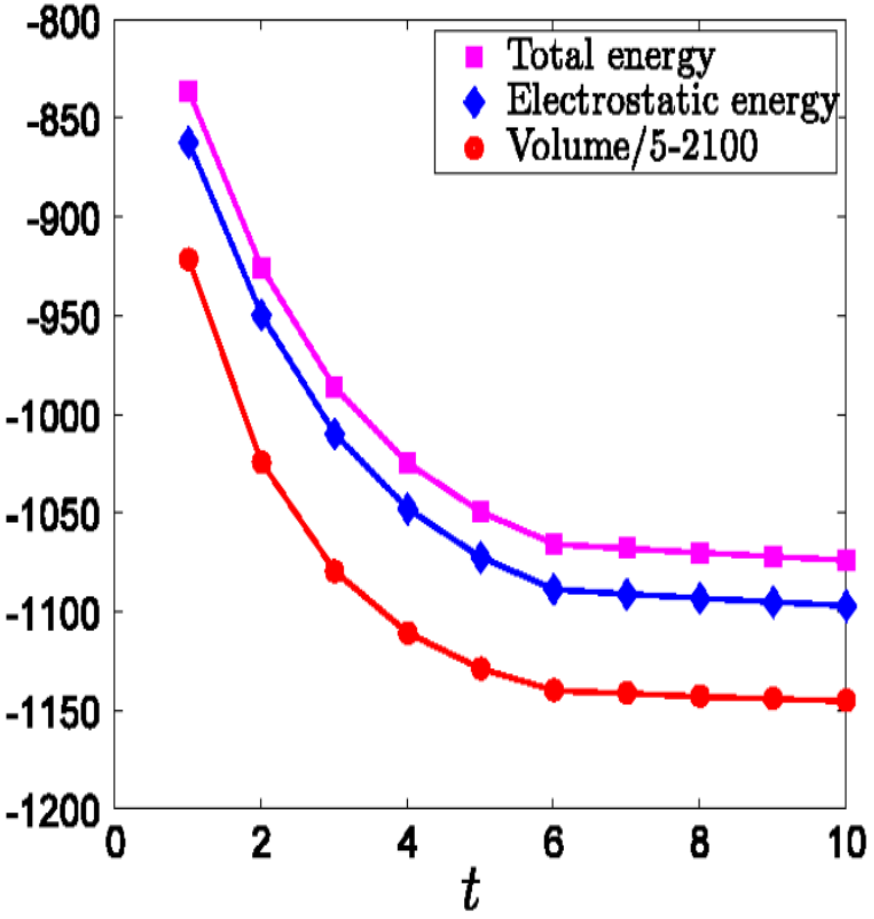

Convergence of the total energy

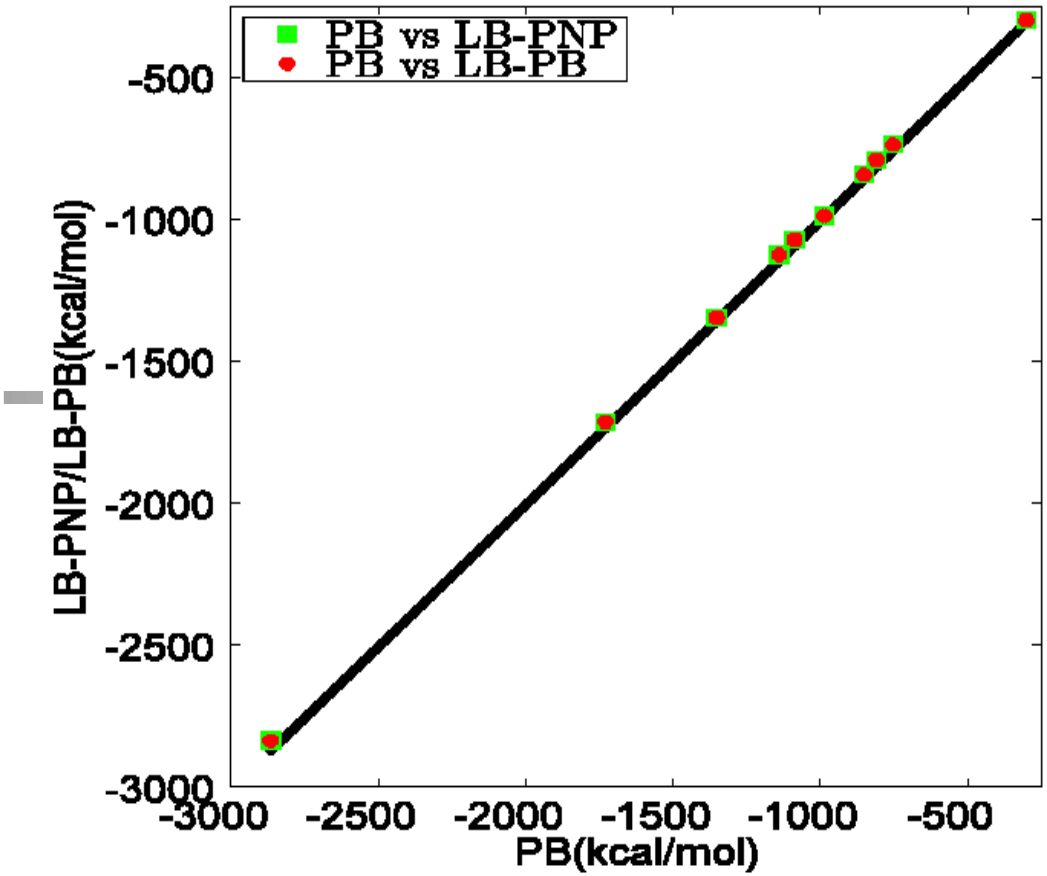

Consistency of three models at equilibrium with 10 proteins

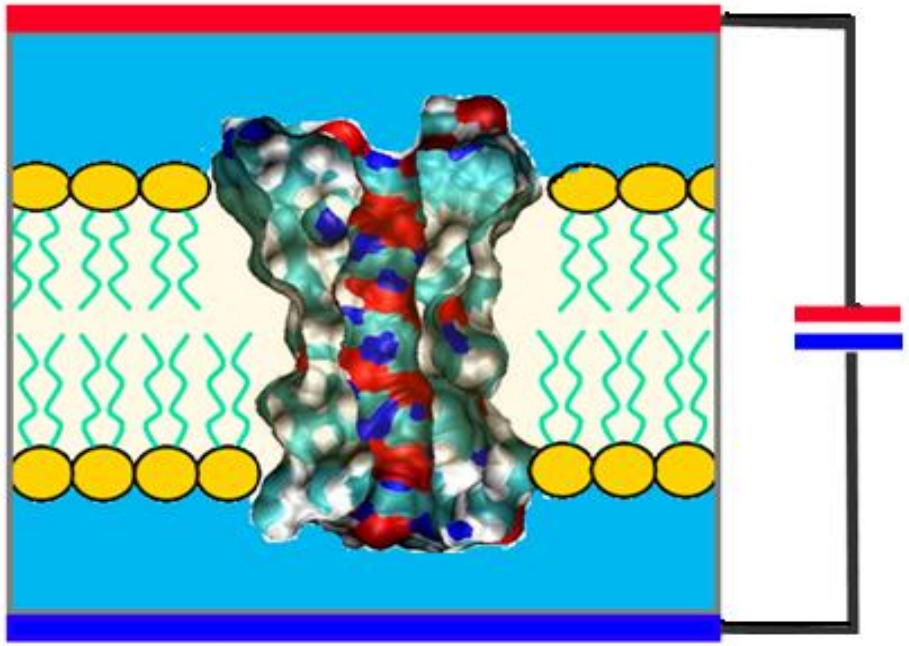

Simulation of Gramicidin A

Laplace-Beltrami and Poisson-Nernst-Planck equations

(Zheng, Chen, Wei, JCP, 2011)

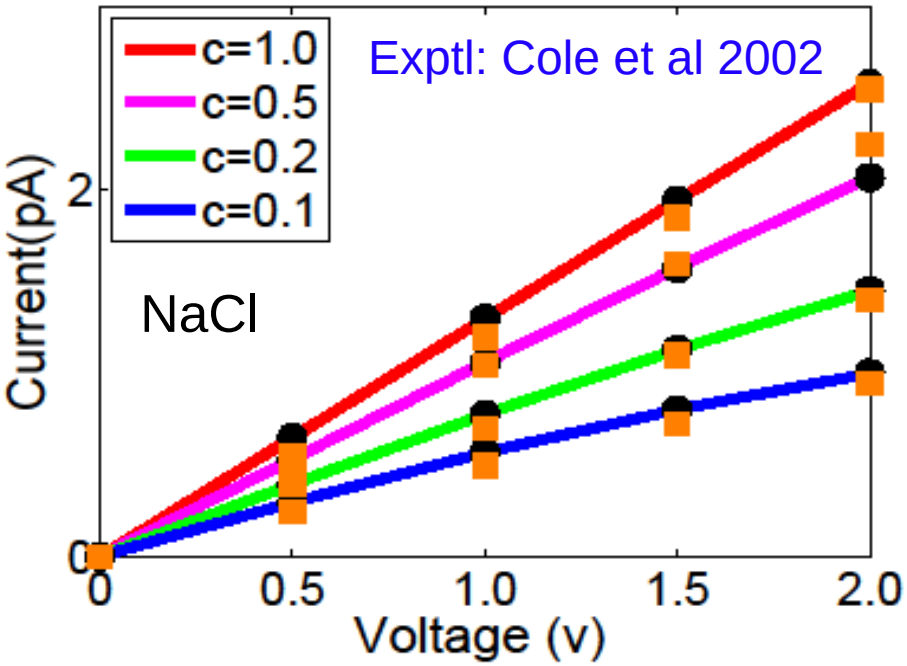

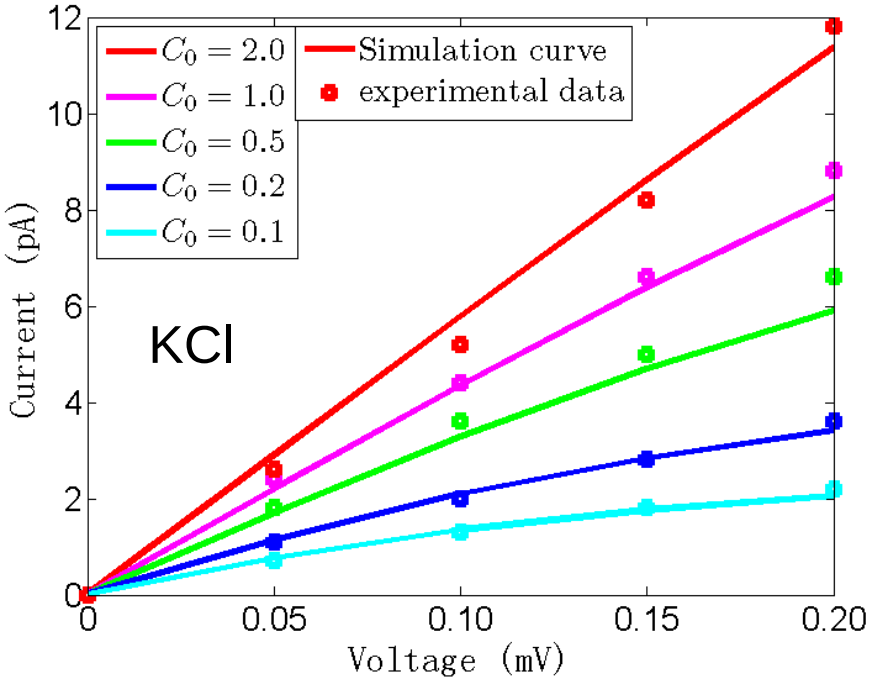

Proton transport

ATP production

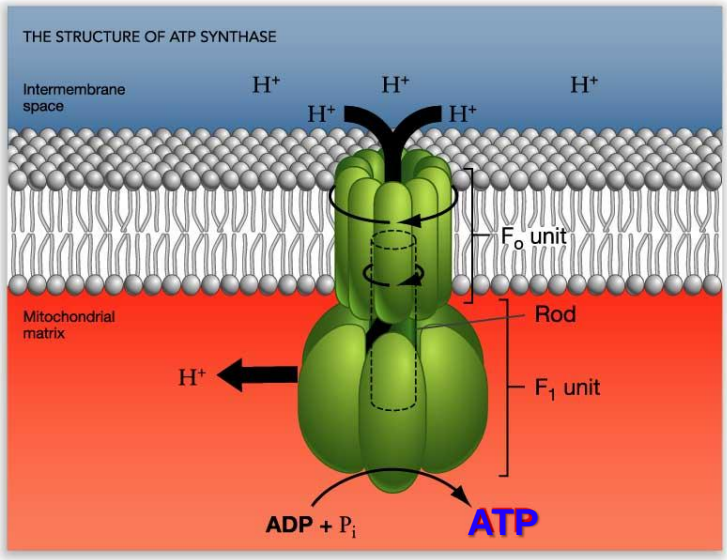

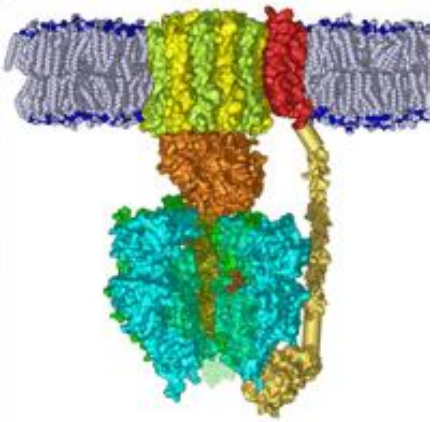

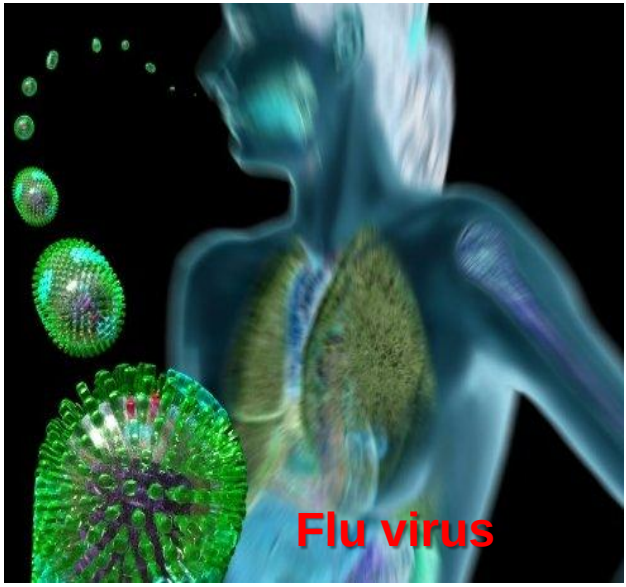

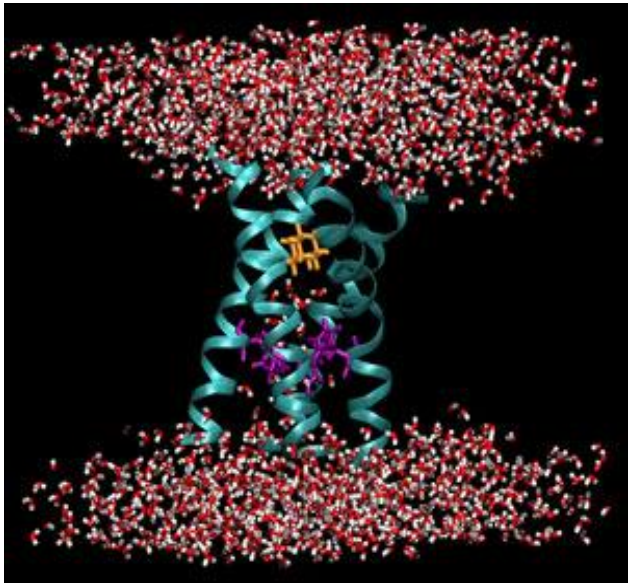

ATP is the energy currency in human body

Influenza M2 proton channel regulates viral replication process in a host cell.

Multiscale model for proton transport

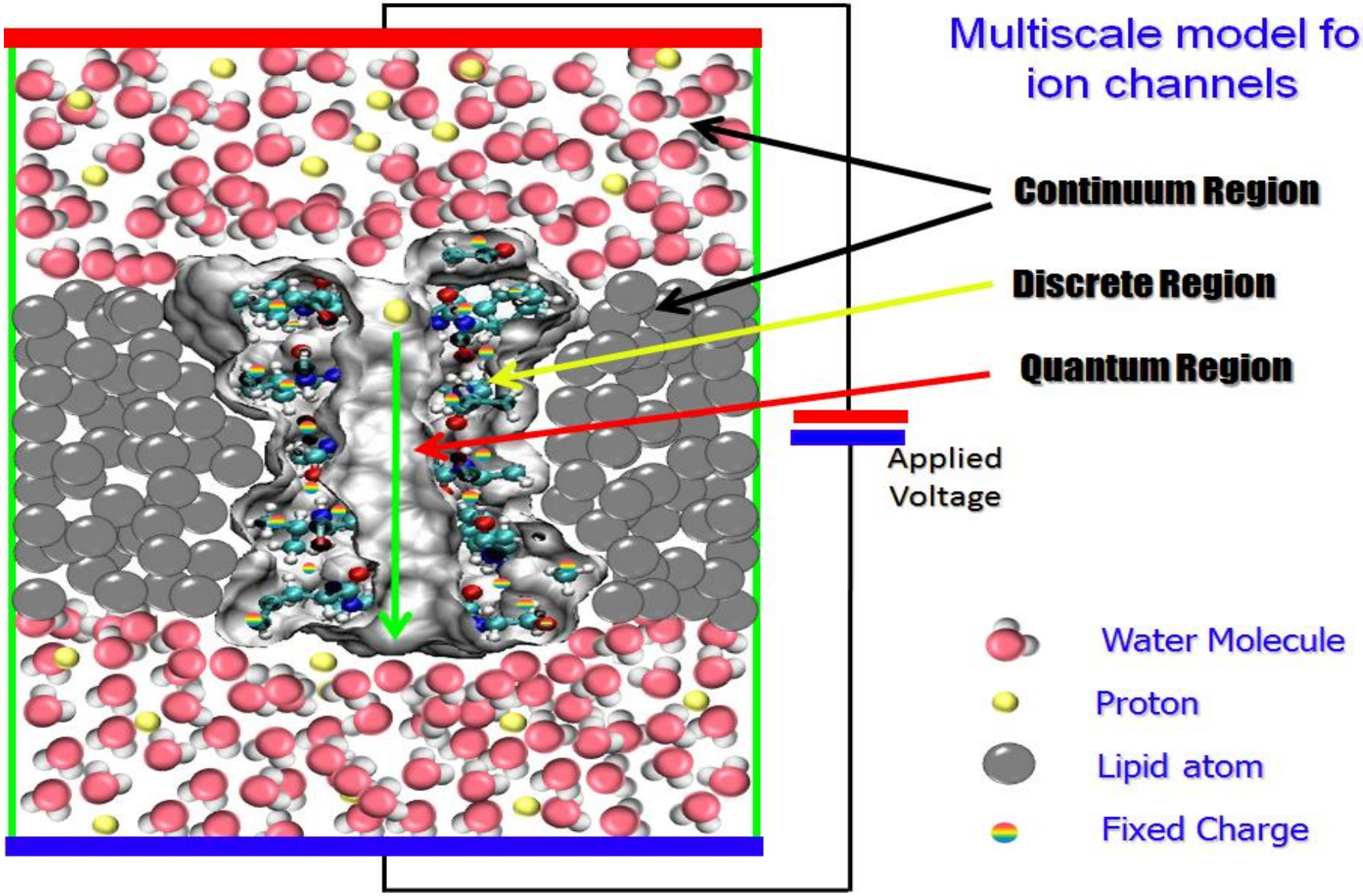

Total energy functional for proton transport

$$G = \int_\Omega G_f d\Omega = \int_\Omega \left[Nonpolar + Electro + QM \right] dr$$

Geometric = area + volume + van der Waals:

$$Nonpolar = \gamma \left| \nabla S \right| + Sp + (1 - S)U$$

Electro = electric field + point charges + proton charges:

$$Electro = \frac{1}{2} \varepsilon(S) \left| \nabla \phi \right|^2 - S \sum_i q_i \delta\left(r - r_i \right) - (1 - S) \phi n$$

QM = kinetic + potential + Lagrange multiplier :

$$QM = (1 - S) \left[\int \left[\frac{\hbar^2 f}{2m} \left| \nabla \psi_E \right|^2 + E_{GC}[n] \right] dE + \lambda \left[\int f \left| \psi_E \right|^2 dE - \frac{N}{V} \right] \right]$$

Proton density: $n = \int \left| \psi_E \right|^2 f dE \qquad f = e^{-(E-\mu)/kT}$

(Chen & Wei, IJNMBE,2011)

Variation of the total free energy functional

$$\frac{\partial S}{\partial t} = \nabla \bullet \left(\frac{\gamma}{|\nabla S|} \nabla S \right) - p + U - \frac{1}{2}\left(\varepsilon_p - \varepsilon_s\right)|\nabla \phi|^2 + \sum_i q_i \delta\left(r - r_i\right) - \phi n - QM / S = 0$$

Generalized Laplace Beltrami equation

$$-\nabla \bullet \left(\varepsilon(S) \nabla \phi\right) = S \sum_i q_i \delta\left(r - r_i\right) + (1 - S) n$$

Generalized Poisson-Boltzmann equation

$$-\frac{\hbar^2}{2m} \nabla^2 \psi_E + \left(U_{GC}[n] - q\phi\right)\psi_E = E_E \psi_E$$

$$where: \qquad U_{GC}[n] = \frac{\delta E_{GC}[n]}{\delta n}$$

Generalized Kohn-Sham equation

with Boltzmann statistics and scattering boundary conditions

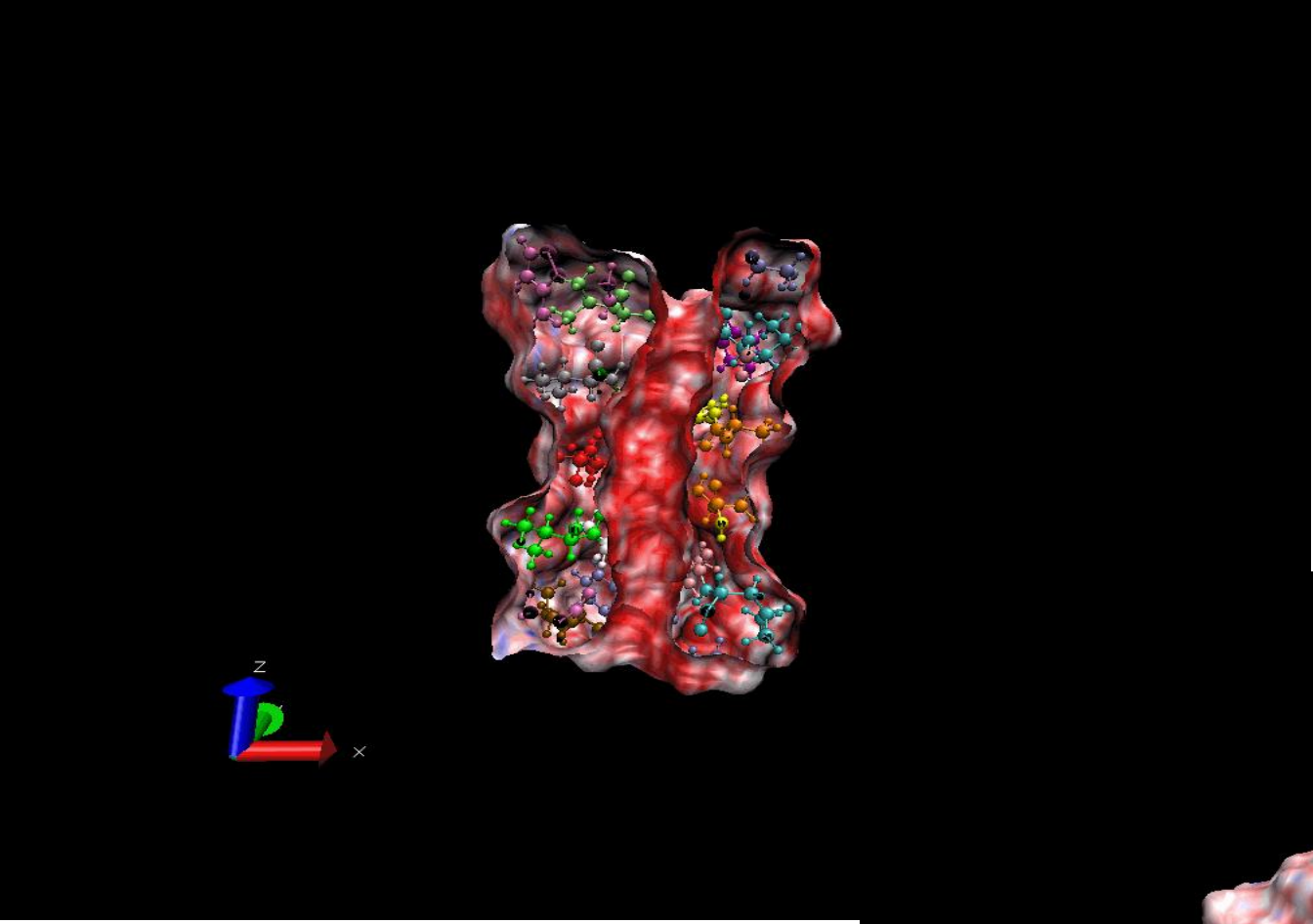
Z
X

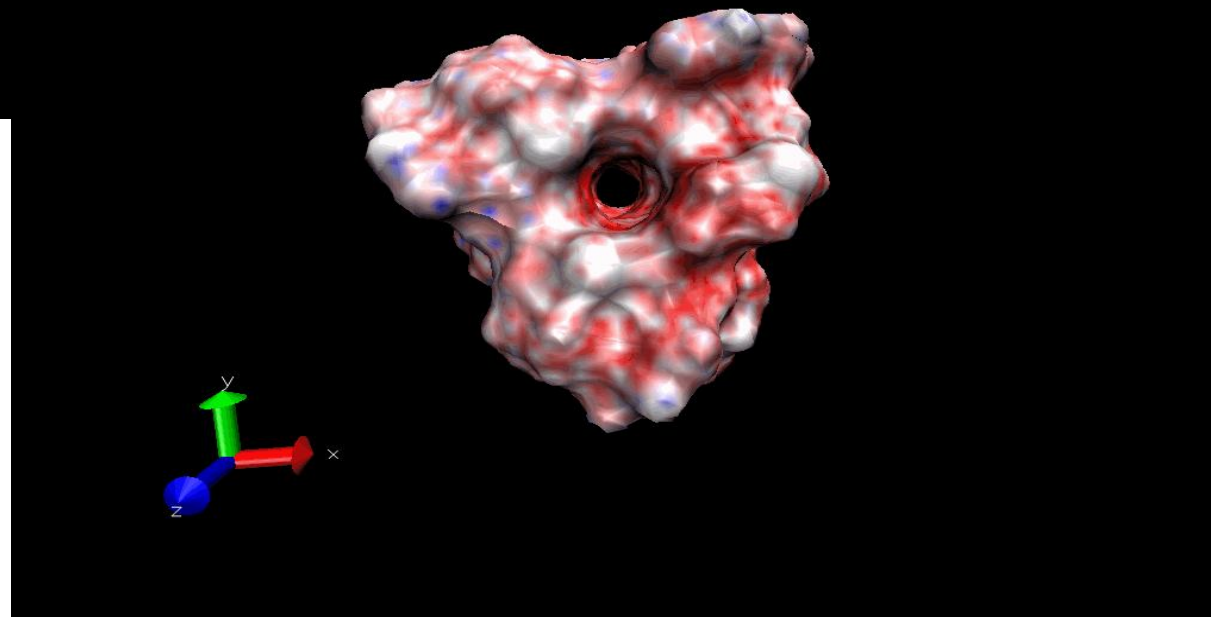
Y
X
Z

Simulation of Gramicidin A

Laplace-Beltrami and Kohn-Sham equations

(Chen, Wei, CiCP, 2011)

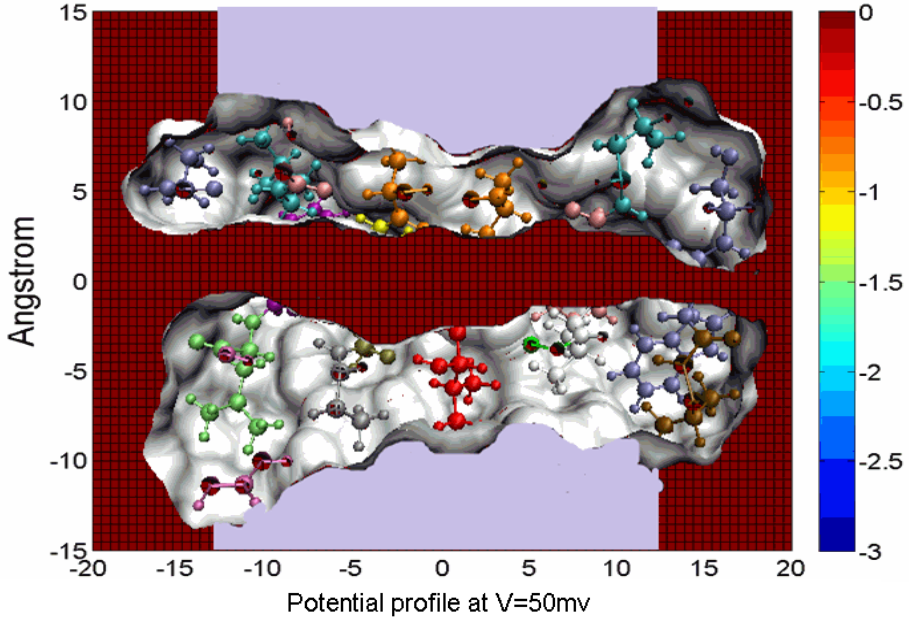

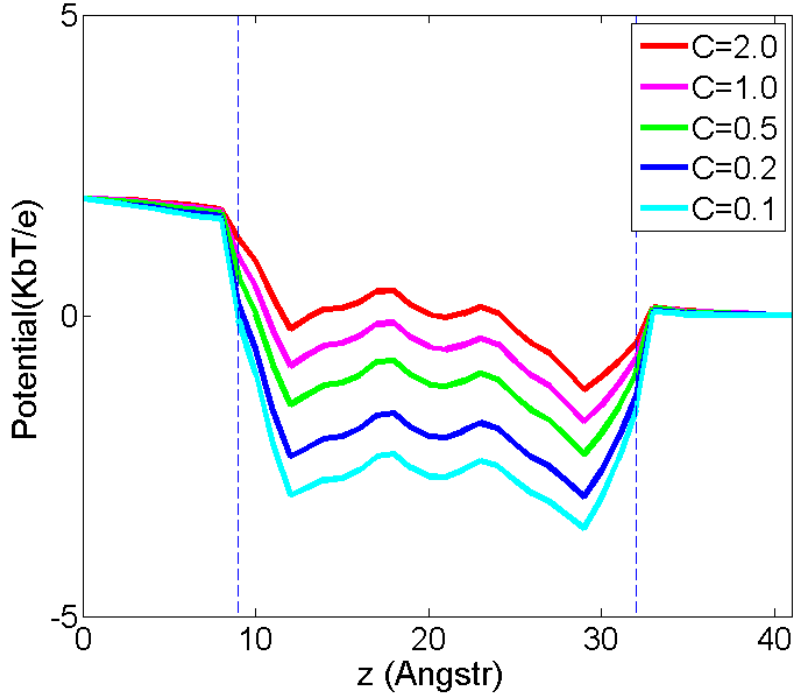

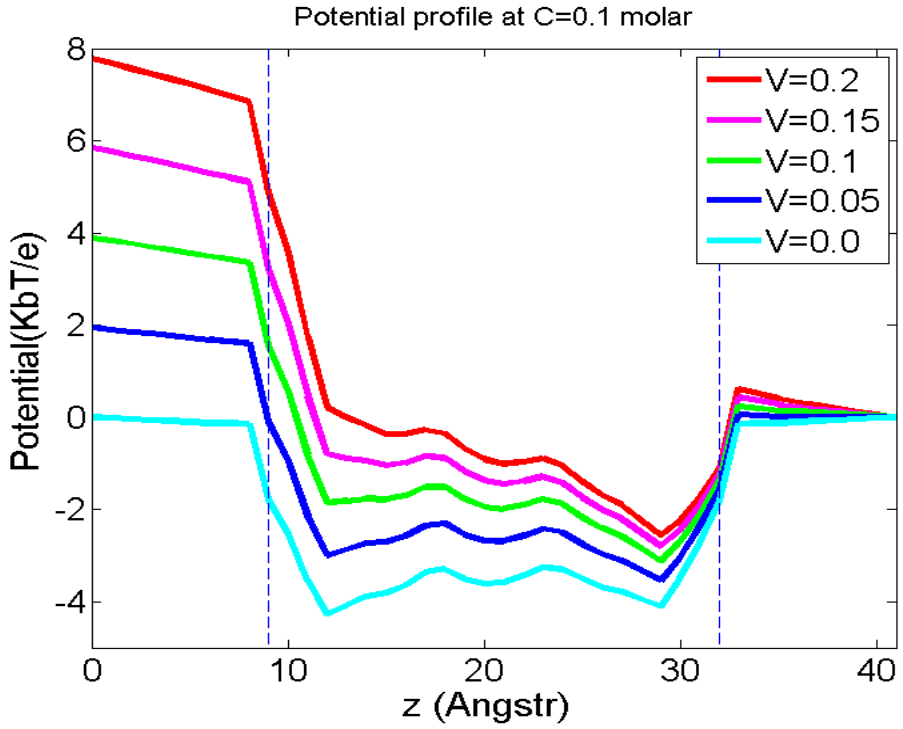

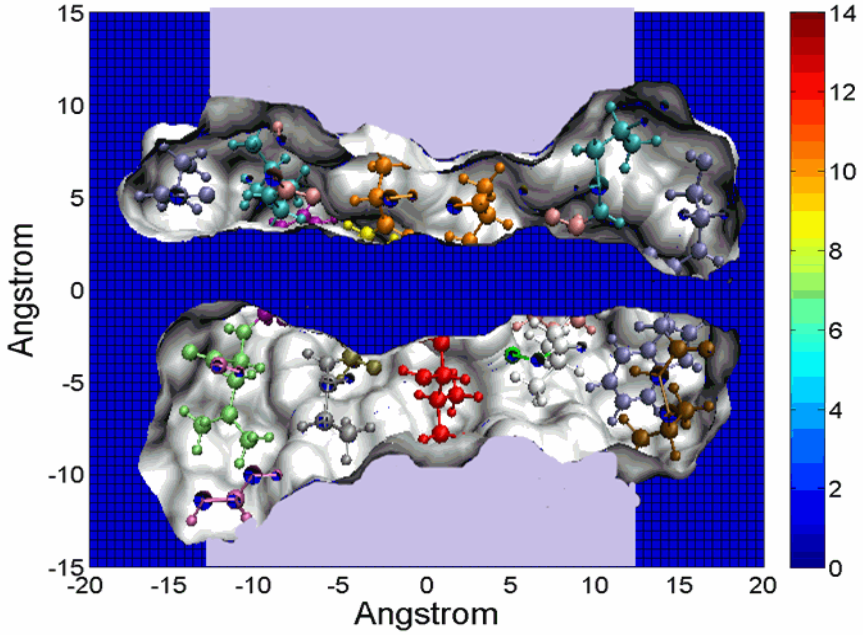

Simulation of Gramicidin A

Laplace-Beltrami and Kohn-Sham equations

(Chen, Wei, CiCP, 2011)

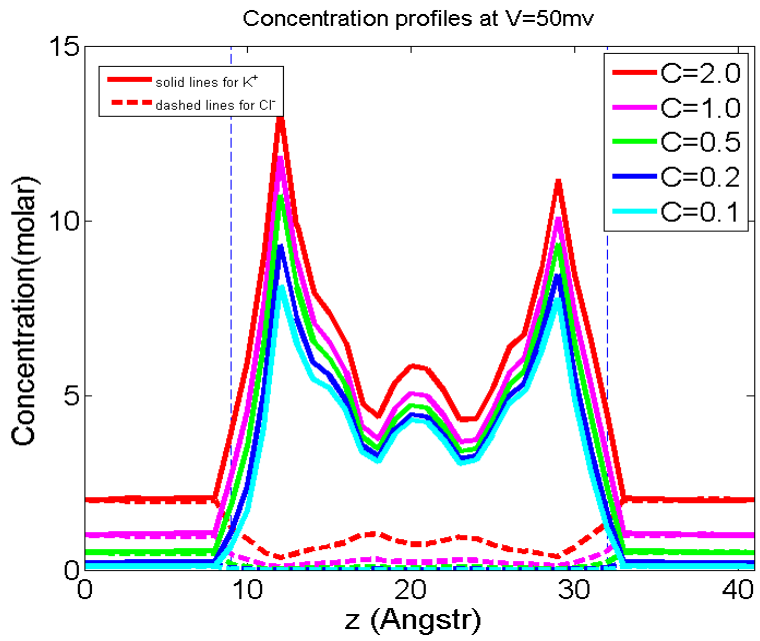

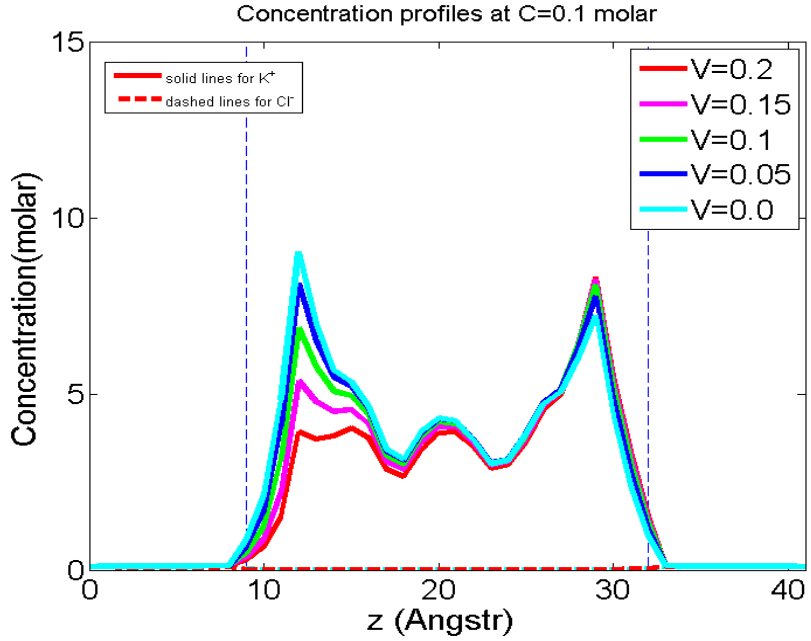

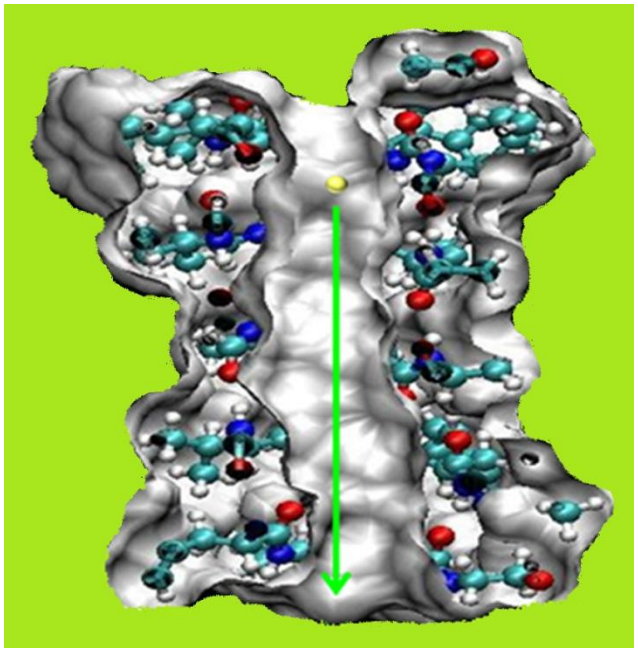

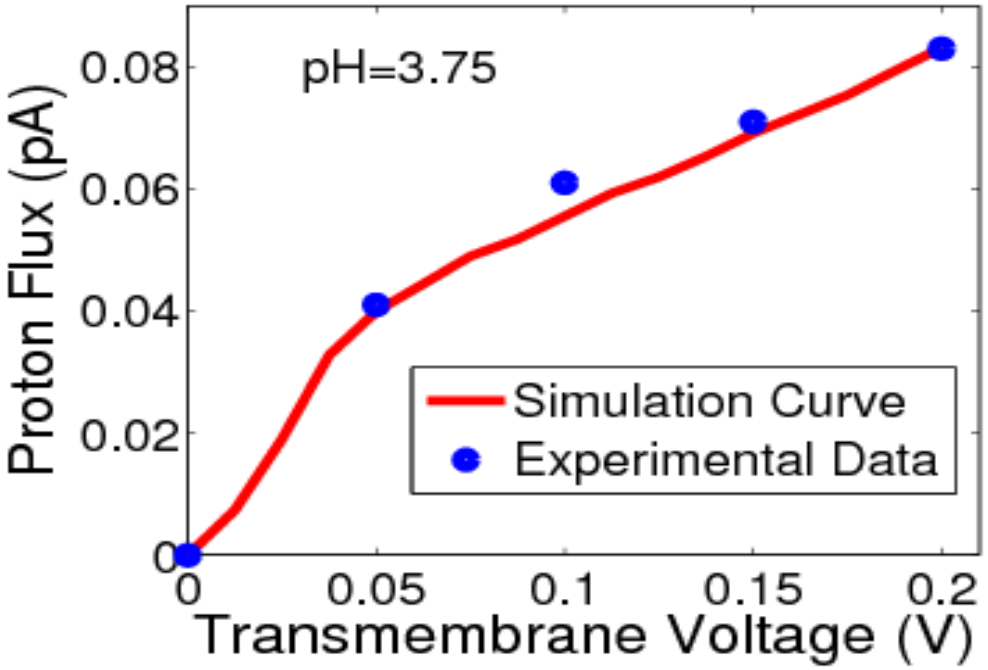

Proton transport of Gramicidin A

(Expl: Eisenman et al., 1980)

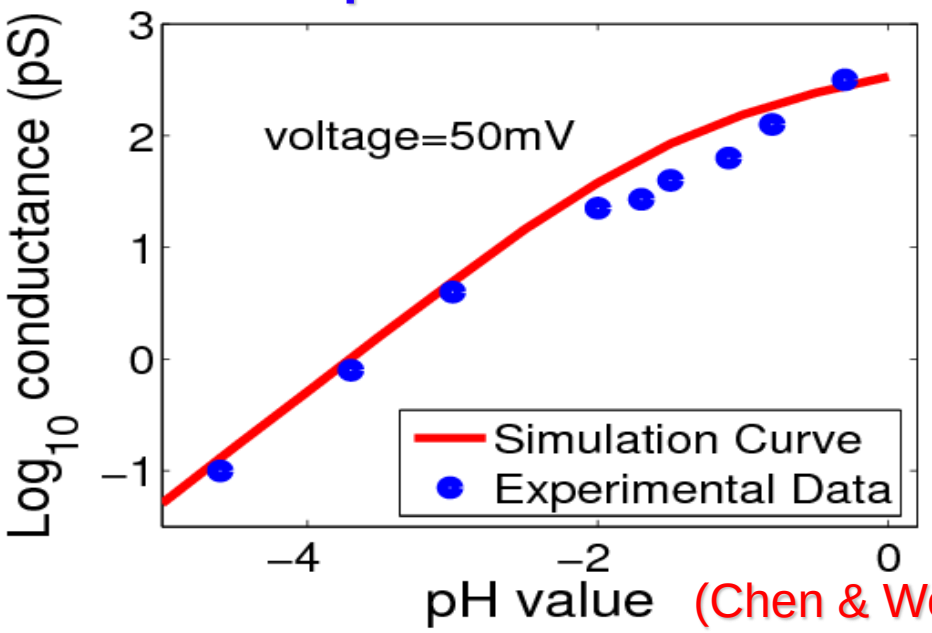

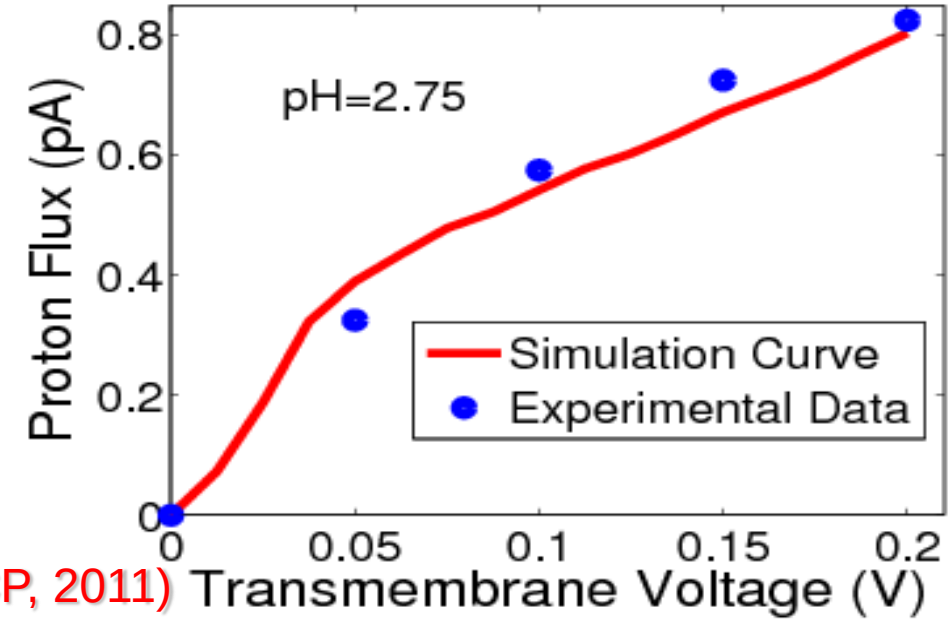

(Chen & Wei, CiCP, 2011)

To improve variational multiscale models

- **Need to describe the configurational changes due to receipt binding**
- **Need to account for the structural response to the ion permeation**
- **Need to reflect water flow due to the cellular material balance**
- **Need to account for ion-ion and ion-water correlations**

Electro-Chem-Fluid-MM model

$$G = \iiint \left[Nonpolar + Electro + Chemical + Fluid + MM \right] dxdzdt$$

$$G_{Nonpolar} = \gamma \left| \nabla S \right| + Sp + (1-S) \sum_{\alpha} n_{\alpha} U_{\alpha}$$

$$G_{Electro} = S \left[\phi \rho_m - \frac{\varepsilon_m}{2} \left| \nabla \phi \right|^2 \right] + (1-S) \left[\phi \sum_{\alpha} n_{\alpha} q_{\alpha} - \frac{\varepsilon_s}{2} \left| \nabla \phi \right|^2 \right]$$

$$G_{Chemical} = (1-S) \sum_{\alpha} n_{\alpha} \left[\mu_{0\alpha} + kT \left(\ln \frac{n_{\alpha}}{n_{\alpha 0}} - 1 \right) \right]$$

$$G_{Fluid} = -(1-S) \left[\rho_s \frac{v^2}{2} - p + \frac{\mu}{8} \int^t \left(\frac{\partial v_i}{\partial x_j} + \frac{\partial v_j}{\partial x_i} \right)^2 dt' \right]$$

$$G_{MM} = -S \sum \left[\rho_j \frac{\dot{z}_j^2}{2} - U(z) \right]$$

(Wei, BMB, 2010)

Generalized Navier-Stokes Equation

$$\rho_s\left(\frac{\partial v}{\partial t}+v\cdot\nabla v\right)=-\nabla p+\frac{1}{1-S}\nabla\bullet(1-S)T+F$$

$$F=\frac{S}{1-S}\left(-\nabla p-\frac{1-S}{S}\nabla\left(\rho_s U_s+\sum_\alpha n_\alpha q_\alpha\phi\right)+\frac{\rho_m}{S}\nabla(S\phi)\right)$$

$$\nabla\cdot v=0$$

Generalized Newton equation for molecular dynamics

$$\rho_j\frac{d^2z_j}{dt^2}=f_{SSI}^j+f_{RF}^j+f_{PI}^j$$

$$f_{SSI}^j=-\frac{1-S}{S}\nabla_j(\rho_s U_s)$$

$$f_{RF}^j=\frac{\rho_m}{S}\nabla_j(S\phi)-\frac{1-S}{S}\nabla_j n_\alpha q_\alpha\phi$$

$$f_{PI}^j=-\nabla_j U(z)$$

Generalized Poisson Equation

$$-\nabla \bullet \varepsilon(S)\nabla\phi = S\rho_m + (1-S)\sum n_\alpha q_\alpha$$

$$\varepsilon(S) = S\varepsilon_m + (1-S)\varepsilon_s$$

Electrochemical potential

$$\frac{\delta G}{\delta n_\alpha} \Rightarrow \qquad \mu_\alpha = \mu_{0\alpha} + kT\ln\frac{n_\alpha}{n_{\alpha 0}} + q_\alpha\phi + U_\alpha$$

Nernst-Planck equation

$$J_\alpha = -D_\alpha n_\alpha \nabla\frac{\mu_\alpha}{kT}, \qquad \frac{\partial n_\alpha}{\partial t} + v \bullet \nabla n_\alpha = -\nabla \bullet J_\alpha$$

$$\frac{\partial n_\alpha}{\partial t} + v \bullet \nabla n_\alpha = \nabla \bullet \left[D_\alpha \left(\nabla n_\alpha + \frac{q_\alpha n_\alpha}{kT} \nabla\left[\phi + U_\alpha\right] \right) \right]$$

Generalized Laplace-Beltrami equation

$$\frac{\partial S}{\partial t} = |\nabla S| \left[\nabla \bullet \frac{\gamma \nabla S}{|\nabla S|} + V_{LB} \right]$$

$$V_{LB} = -p + \sum_{\alpha} n_{\alpha} U_{\alpha} - \rho_m \phi + \frac{\varepsilon_m}{2} |\nabla \phi|^2 + \sum_{\alpha} n_{\alpha} q_{\alpha} \phi - \frac{\varepsilon_s}{2} |\nabla \phi|^2$$

$$+ \sum_{\alpha} n_{\alpha} \left[\mu_0 + kT \ln \left(\frac{n_{\alpha}}{n_{\alpha 0}} - 1 \right) \right]$$

$$- \left[\rho_s \frac{v^2}{2} - p + \frac{\mu}{8} \int^t \left(\frac{\partial v_i}{\partial x_j} + \frac{\partial v_j}{\partial x_i} \right)^2 dt' \right]$$

$$+ \sum \left[\rho_j \frac{\dot{z}_j^2}{2} - U(z) \right]$$

Multiscale Molecular dynamics

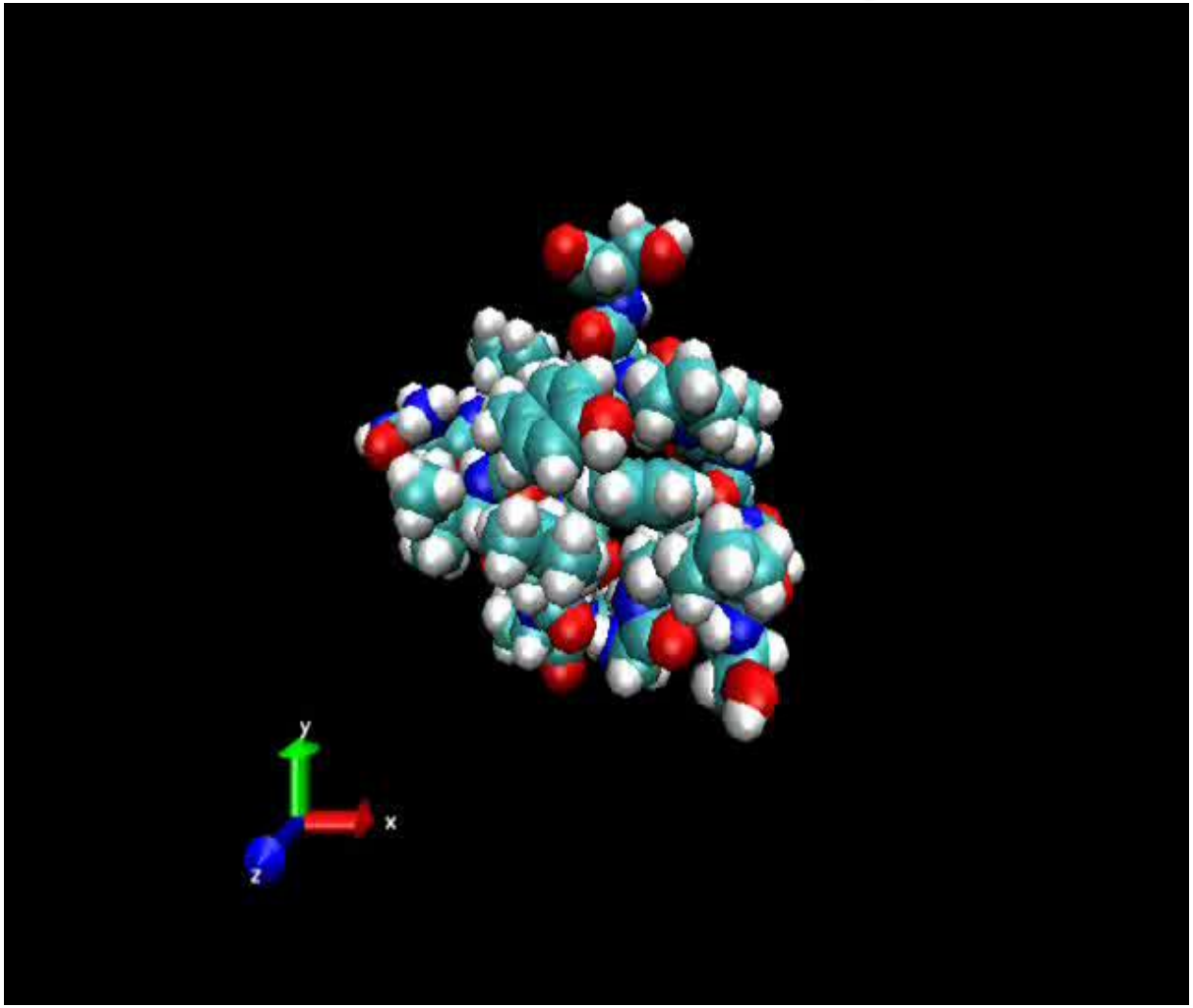

Multiscale MD of Trp-cage miniprotein (1L2Y)

(Geng & Wei, JCP, 2011)

Coupling of fluid & molecular dynamics

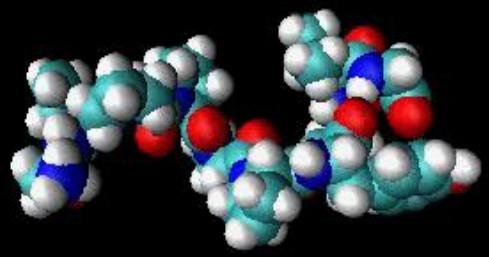

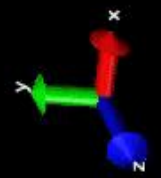

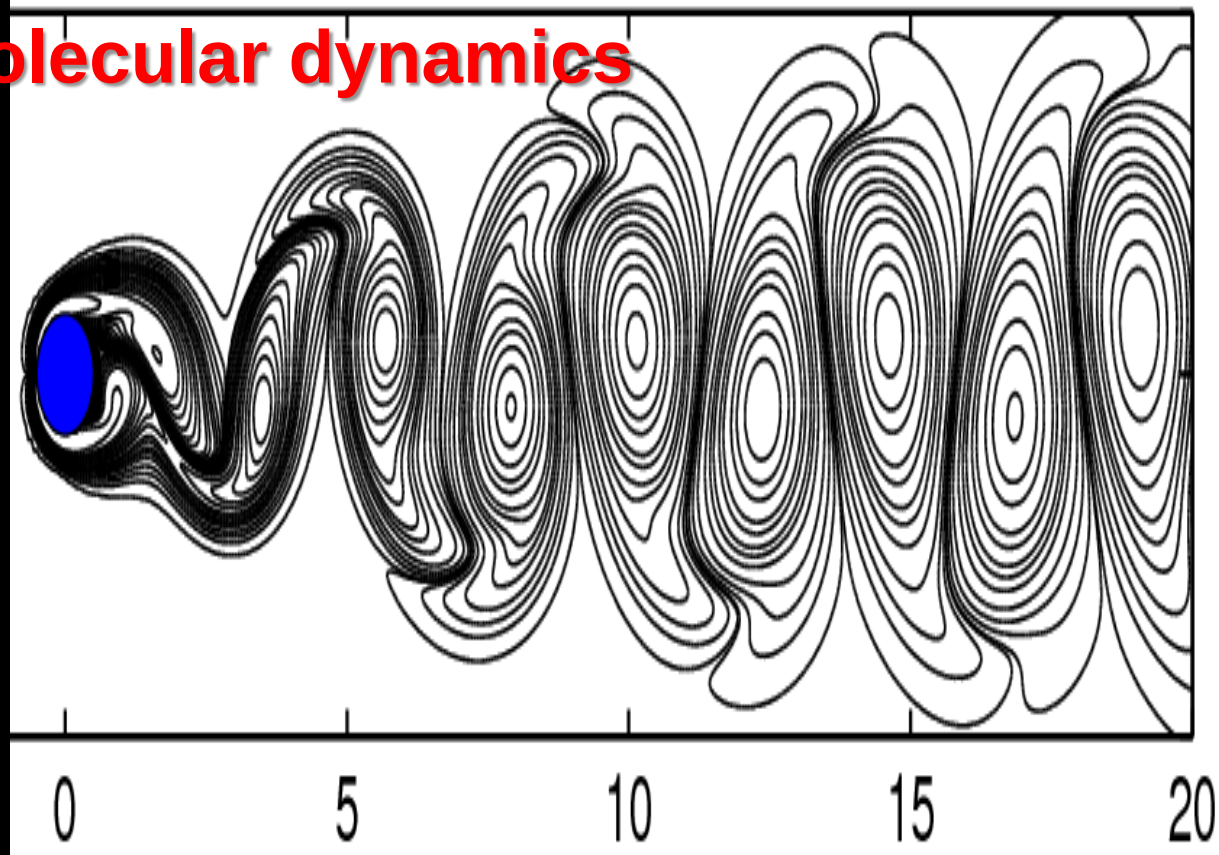

Work in progress

N Baker
(PNNL)
P Bates
(MSU)
M Feig
(MSU)
Y Tong
(MSU)
G Wang
(VPI)
J Wang
(NSF)
Y Wang
(MSU)
X Ye
(UKLR)
Shan Zhao
Alabama
Y Zhou
Colorado S
W Geng
Alabama
S Yang
City U KH
Duan Chen
Ohio State
Zhan Chen
Minnesota
S.N. Yu
Boston
Y.H. Sun
Denver